Interactions of the DNA Polymerase X from African Swine Fever Virus with Gapped DNA Substrates. Quantitative Analysis of Functional Structures of the Formed Complexes†

Maria J. Jezewska, Paul J. Bujalowski, and Wlodzimierz Bujalowski*

Department of Biochemistry and Molecular Biology, Department of Obstetrics and Gynecology, The Sealy Center for Structural Biology, Sealy Center for Cancer Cell Biology, The University of Texas Medical Branch at Galveston, 301 University Boulevard, Galveston, Texas 77555-1053

Received April 10, 2007; Revised Manuscript Received June 15, 2007

ABSTRACT: Energetics and specificity of interactions between the African swine fever virus polymerase X and gapped DNA substrates have been studied, using the quantitative fluorescence titration technique. Stoichiometries of pol X complexes, with the DNA substrates, are higher than suggested by NMR studies. This can be understood in the context of the functionally heterogeneous organization of the total DNA-binding site of pol X, which is composed of two DNA-binding subsites. The enzyme forms two different complexes with the gapped DNAs, differing dramatically in affinities. In the high-affinity complex, pol X engages the total DNA-binding site, forming the gap complex, while in the low-affinity the enzyme binds to the dsDNA parts of the gapped DNA, using only one of the DNA-binding subsites. As a result, the net number of ions released in the gap complex formation is significantly larger than in the binding of the dsDNA part. In the presence of Mg^{+2}, pol X shows a strong preference for the ssDNA gaps having one and two nucleotides. Recognition of the short gaps already occurs in the ground state of the enzyme−DNA complex. Surprisingly, the specific structure necessary to recognize the short gaps is induced by magnesium binding to the enzyme. In the absence of Mg^{+2}, pol X looses its selectivity for short ssDNA gaps. Pol X binds gapped DNAs with considerable cooperative interactions, which increase with the decreasing gap size. The functional implications of these findings for ASFV pol X activities are discussed.

The African swine fever virus (ASFV[1]) is the subject of intensive studies as the factor responsible for acute hemorrhagic fever, which has a mortality approaching 100%, in domestic pigs (*1*−*5*). Interestingly, the DNA genome of ASFV virus encodes two DNA polymerases (*4*−*7*): a replicative polymerase which belongs to the eukaryotic family B enzymes and another polymerase, a member of the pol X family, referred to as ASFV pol X (*4*−*9*). ASFV pol X shows significant functional similarities to other DNA-repair polymerases that include distributive DNA synthesis on template-primer DNA substrates and efficient filling of single nucleotide gaps (*5*−*7*). This spectrum of functional activities and the fact that the ASFV genome codes for another strictly replicative DNA polymerase along with several enzymes that perform most of the base excision repair (BER) pathway indicate that the ASFV pol X is involved in the repair processes of the viral DNA, damaged by the host reaction to the viral infection (*8*−*14*).

With a molecular weight of ∼20000, ASFV pol X is currently the smallest known DNA polymerase. NMR studies of the ASFV pol X show a structure which is very different from the structures of other known replicative or repair DNA polymerases (*15*−*17*). Pol X is only built of the palm domain, which includes the first 105 amino acids from the N-terminus of the protein and the C-terminal domain, built of the remaining 69 amino acid residues. The NMR structure of the enzyme is depicted in Figure 1 (*15*). The active site of the DNA synthesis resides in the palm domain where the triad of invariant aspartate residues, typical for DNA polymerases, is located (*15*, *16*). Moreover, the palm domain contains a positively charged helix, αC, located at the surface of the domain. Similarly, the C-terminal domain contains a highly positively charged helix, αE. These structural features suggest that both the palm and the C-terminal domain are engaged in interactions with the DNA (*15*, *16*, *18*).

A puzzling problem in the DNA recognition mechanism, by a DNA repair polymerase, is the fact that the enzyme must recognize the damaged DNA containing a small ssDNA gap, in the context of the large excess of the dsDNA (*18*−*25*). Our recent quantitative studies shed light on the complex interactions of the ASFV pol X with the nucleic acid (*18*). The total site-size of the pol X−ssDNA complex is 16 ± 2 nucleotide residues, surprisingly large for such a small protein. The total ssDNA-binding site has a complex heterogeneous structure. It contains the proper ssDNA-binding site, a structurally and functionally separated area, characterized by the high nucleic acid affinity, which encompasses only 7 ± 1 nucleotides. On the other hand, the

† This work was supported by NIH Grant GM-58675 (to W.B.).

* Send correspondence to this author: Department of Biochemistry and Molecular Biology, The University of Texas Medical Branch at Galveston, 301 University Boulevard, Galveston, TX 77555-1053. Tel: (409) 772-5634. Fax: (409) 772-1790. E-mail: wbujalow@utmb.edu.

[1] Abbreviations: ASFV, African swine fever virus; DTT, dithiothreitol; ssDNA, single-stranded DNA; dsDNA, double-stranded DNA; MCT method, macromolecular competition titration method; BER, base excision repair.

10.1021/bi700677j CCC: $37.00
Published on Web 10/17/2007

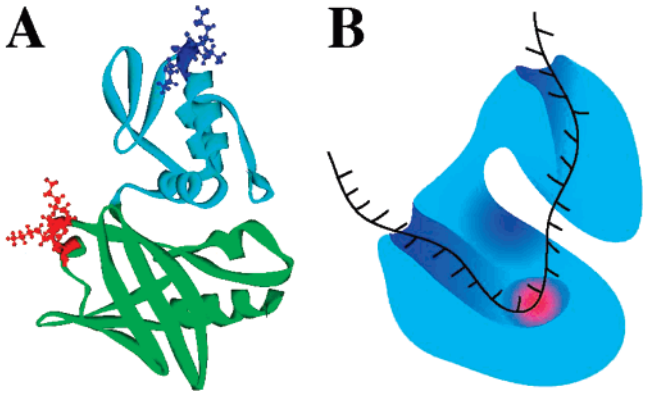

FIGURE 1: (a) Three-dimensional structure of the ASFV pol X obtained by NMR studies (*15*). The first 105 amino acid residues from the N-terminus of the protein constitute the palm domain, while the remaining 69 amino acid residues form the C-terminal domain of the enzyme. The domains are marked in green and turquoise colors, respectively. Also, the lysine residues, 59, 60, and 63 in the palm domain, and the lysine residues 131, 132, and 133 contained in the αC helix the αE helix of the palm and the C-terminal domain, respectively, are selected and marked in red and blue colors, respectively. (b) Schematic representation of the ASFV pol X domain structure with the total DNA-binding site of the polymerase engaged in the complex with the ssDNA (*18*). The darker areas mark the two presumed DNA-binding subsites. The small red area indicates the location of active site of the enzyme.

enzyme can engage an additional binding area in interactions with the DNA at a distance of ~7−8 nucleotides from the proper site. However, in complexes with the longer ssDNA oligomers, pol X does not form different binding modes where the enzyme engages only one of its DNA-binding subsites in interactions with the DNA. Such different binding modes were observed for the mammalian pol β, which belongs to the same DNA polymerase family (*19*−*25*). This different behavior indicates that both DNA-binding areas, within the total DNA-binding site of pol X, are less autonomous than observed for pol β and/or that the enzyme cannot adjust its orientation on the ssDNA to enable the binding of another polymerase molecule (*19*−*26*).

Interactions of a DNA polymerase, with the DNA, play a vital role in the function of the enzyme as one of the major elements, which determine the degree of fidelity of the DNA synthesis, as the polymerase complex with the DNA constitutes the binding and recognition site for dNTPs (*27*−*29*). Moreover, in the case of a DNA repair polymerase, elucidation of the enzyme interactions with the nucleic acid is of paramount importance for understanding the recognition mechanism of the damaged DNA (*18*−*26*, *30*−*33*). How a polymerase, with such a simplified structure as the ASFV pol X, recognizes ssDNA gaps in the damaged DNAs is unknown. In spite of its paramount importance for understanding the DNA recognition process by a DNA repair polymerase and the ASFV pol X in particular, the direct and quantitative analyses of pol X interactions with the gapped DNA have not been addressed. The fundamental aspects of these interactions, like stoichiometries, intrinsic affinities, cooperativities, and the role of the size of the ssDNA gap in the recognition process, are unknown.

MATERIALS AND METHODS

Reagents and Buffers. All chemicals were reagent grade. All solutions were made with distilled and deionized >18 MΩ (Milli-Q Plus) water. The standard buffer C is 10 mM sodium cacodylate adjusted to pH 7.0 with HCl and 10% glycerol.

ASFV Pol X. The plasmid harboring the gene of the ASFV pol X was a generous gift of Dr. Maria L. Salas (Universidad Autonoma, Madrid, Spain). Isolation and purification of the protein was performed, with slight modifications, as described (*6*, *7*, *18*). The protein was >98% pure as judged by SDS acrylamide gel electrophoresis with Coomasie Brilliant Blue staining. The concentration of the protein was spectrophotometrically determined using the extinction coefficient, $\epsilon_{280} = 1.541 \times 10^4$ cm^{-1} M^{-1}, obtained with the approach based on Edelhoch's method (*34*, *35*).

Nucleic Acids. All unmodified and modified ssDNA oligomers were purchased from Midland Certified Reagents (Midland, TX). The modified ssDNA oligomers contain a fluorescent label, fluorescein, introduced through phosphoramidate chemistry. Thus, the fluorescein residue is placed as an analogue of an additional base in each modified DNA. Concentrations of all ssDNA oligomers have been spectrophotometrically determined (*30*−*33*, *36*−*40*).

Fluorescence Measurements. Steady-state fluorescence titrations were performed using the SLM-AMINCO 8100C with polarizers were placed in excitation and emission channels and set at 90° and 55° (magic angle), respectively (*30*−*33*, *36*−*44*). The binding was followed by monitoring the fluorescence of the nucleic acid ($\lambda_{ex} = 495$ nm, $\lambda_{em} = 520$ nm). Computer fits were performed using Mathematica (Wolfram, IL) and KaleidaGraph (Synergy Software, PA). The relative fluorescence quenching of the nucleic acid emission, ΔF_{obs}, upon the ASFV pol X binding is defined as $\Delta F_{obs} = (F_0 - F_i)/F_0$, where F_i is the emission of the DNA substrate at a given titration point "*i*", and F_0 is the initial value of the emission of the sample (*25*, *26*, *30*, *33*).

Quantitative Determination of Binding Isotherms and Stoichiometries of the ASFV Pol X−*Gapped DNA Complexes*. In this work, we followed the binding of pol X to the gapped DNA substrates by monitoring the fluorescence quenching, ΔF_{obs}, of the nucleic acid upon the complex formation. Quantitative estimates of the total average degree of binding, $\Sigma\Theta_i$, (number of the ASFV pol X molecules bound per DNA substrate) and the free protein concentration, P_F, have been previously described in detail by us (*26*, *30*−*33*, *36*−*45*). Briefly, the experimentally observed ΔF_{obs} has a contribution from each of the different possible "*i*" complexes of pol X with the DNA. Thus, the observed relative fluorescence quenching is functionally related to $\Sigma\Theta_i$ by

$$\Delta F_{obs} = \sum \Theta_i \Delta F_{i_{max}} \quad (1)$$

where $\Delta F_{i_{max}}$ is the molecular parameter characterizing the maximum fluorescence quenching of the nucleic acid with pol X bound in complex "*i*". The same value of ΔF_{obs}, obtained at two different total nucleic acid concentrations, N_{T_1} and N_{T_2}, indicates the same physical state of the nucleic acid, i.e., the degree of binding, $\Sigma\Theta_i$, and the free protein concentration, P_F, must be the same. The values of $\Sigma\Theta_i$ and P_F are then related to the total protein concentrations, P_{T_1} and P_{T_2}, and the total nucleic acid concentrations, N_{T_1} and N_{T_2}, at the same value of ΔF_{obs}, by

$$\sum\Theta_i = \frac{P_{T_2} - P_{T_1}}{N_{T_2} - N_{T_1}} \quad (2)$$

$$P_F = P_{T_x} - (\sum\Theta_i)N_{T_x} \quad (3)$$

where $x = 1$ or 2 (*26*, *30*−*33*, *36*−*45*). Quantitative determinations of binding isotherms for the ASFV pol X association with unmodified gapped DNA substrates have been performed using the macromolecular competition titration (MCT) method (*26*, *42*).

RESULTS

Binding of the ASFV Pol X to the Gapped DNA Substrates Containing Different Number of Nucleotides in the ssDNA Gap. Our previous studies have shown that binding of the ASFV pol X to the etheno-derivatives of the ssDNA is accompanied by a large nucleic acid fluorescence increase (*18*). A similar large fluorescence increase is observed for the gapped DNA substrates containing etheno-derivatives of adenosine (see below). However, the fluorescence intensity of the etheno-adenosine, when embedded into an oligomer, is significantly diminished (*46*, *47*). As a result, in the case of high-affinity interactions between the ASFV pol X and gapped DNA substrates examined in this work, the concentration of the DNA substrate necessary to perform high-resolution fluorescence titrations makes it very difficult to address both stoichiometries, as well as the intrinsic affinities of the enzyme. On the other hand, we have found that binding of the enzyme to gapped DNAs, containing the fluorescein residue, in place of one of the bases in the ssDNA gap, is accompanied by a large fluorescence quenching of the nucleic acid emission. The high quantum yield of fluorescein provides the required signal to monitor the enzyme-gapped DNA complex formation at experimentally adequate DNA concentrations (*24*, *25*, *30*, *33*).

The gapped DNA substrates, used to examine interactions with ASFV pol X, are depicted in Figure 2. All DNA substrates contain two dsDNA parts each having 10 bps. The length of the dsDNA parts is dictated by the site-size of the proper DNA-binding site of the enzyme, which encompasses 7 ± 1 nucleotides (*18*). The primary structure of the dsDNA parts is identical in all gapped DNAs. The dsDNA parts are separated by the ssDNA gap, which has five, four, three, two, and one nucleotide. The bases of the nucleotide residues in the ssDNA gap are all adenosines with the exception of the residue at the 5′ end of the gap that is replaced by fluorescein. It provides the signal to monitor the interactions. The size of the ssDNA gap is referred to the size that includes the analogue.

Fluorescence titrations of the DNA substrate, having a ssDNA gap with five nucleotides (Figure 2; substrate A), with the ASFV pol X at two different nucleic acid concentrations, in the standard buffer C, containing 198 mM NaCl and 1 mM $MgCl_2$, are shown in Figure 3a. The relative quenching of the nucleic acid fluorescence reaches the value of 0.58 ± 0.03 at saturation. To quantitatively obtain the total average degree of binding, $\sum\Theta_i$, independent of any assumption about the relationship between the observed signal and $\sum\Theta_i$, the titration curves in Figure 3a have been analyzed, using the approach outlined in Materials and Methods (*26*, *30*−*33*, *36*−*45*). Figure 3b shows the dependence of the observed relative fluorescence quenching, ΔF, as a function of the total average degree of binding, $\sum\Theta_i$, of the ASFV pol X on the considered DNA substrate. The plot is, within experimental accuracy, linear. We could determined the total average degree of binding up to ~1.6. Short extrapolation of $\sum\Theta_i$ to the maximum fluorescence quenching, $\Delta F_{max} = 0.58 \pm 0.03$, provides a value of $\sum\Theta_i = 2 \pm 0.2$. Thus, at saturation, two ASFV pol X molecules bind to the gapped DNA substrate containing 5 nucleotides in the gap.

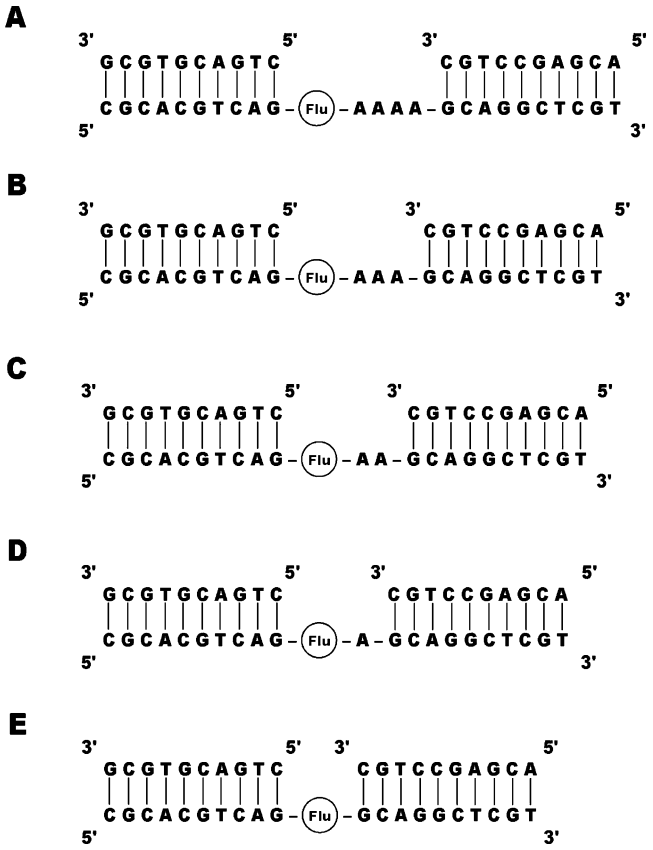

FIGURE 2: A series of gapped DNA substrates that are used to examine the interactions with the ASFV pol X. Each DNA substrate has two dsDNA parts at the 5′ end (downstream from the primer) and at the 3′ end (primer location) of the template strand, which are identical in all substrates. The dsDNA parts are separated by the ssDNA gap containing five (A), four (B), three (C), two (D), and one (E) nucleotide. The template strand contains a fluorescent label, fluorescein, introduced through phosphoramidate chemistry at the 5′ end of the ssDNA gap. Thus, the fluorescein residue, which provides the signal to monitor the interactions with the ASFV pol X, is placed as an analogue of an additional base in each gapped DNA substrate.

Such large stoichiometry is very surprising in light of the fact that the ASFV pol X does not form different binding modes with the ssDNA (*18*). Fluorescence titrations of the DNA substrate, having a ssDNA gap of two nucleotide residues in length (Figure 2; substrate D), with the ASFV pol X at two different nucleic acid concentrations are shown in Figure 3c. The relative quenching of the nucleic acid fluorescence reaches the value of 0.53 ± 0.04 at saturation, which is similar, although not identical, to the value observed for the substrate with the ssDNA gap containing five nucleotides. Figure 3d shows the dependence of the observed relative fluorescence quenching as a function of the total

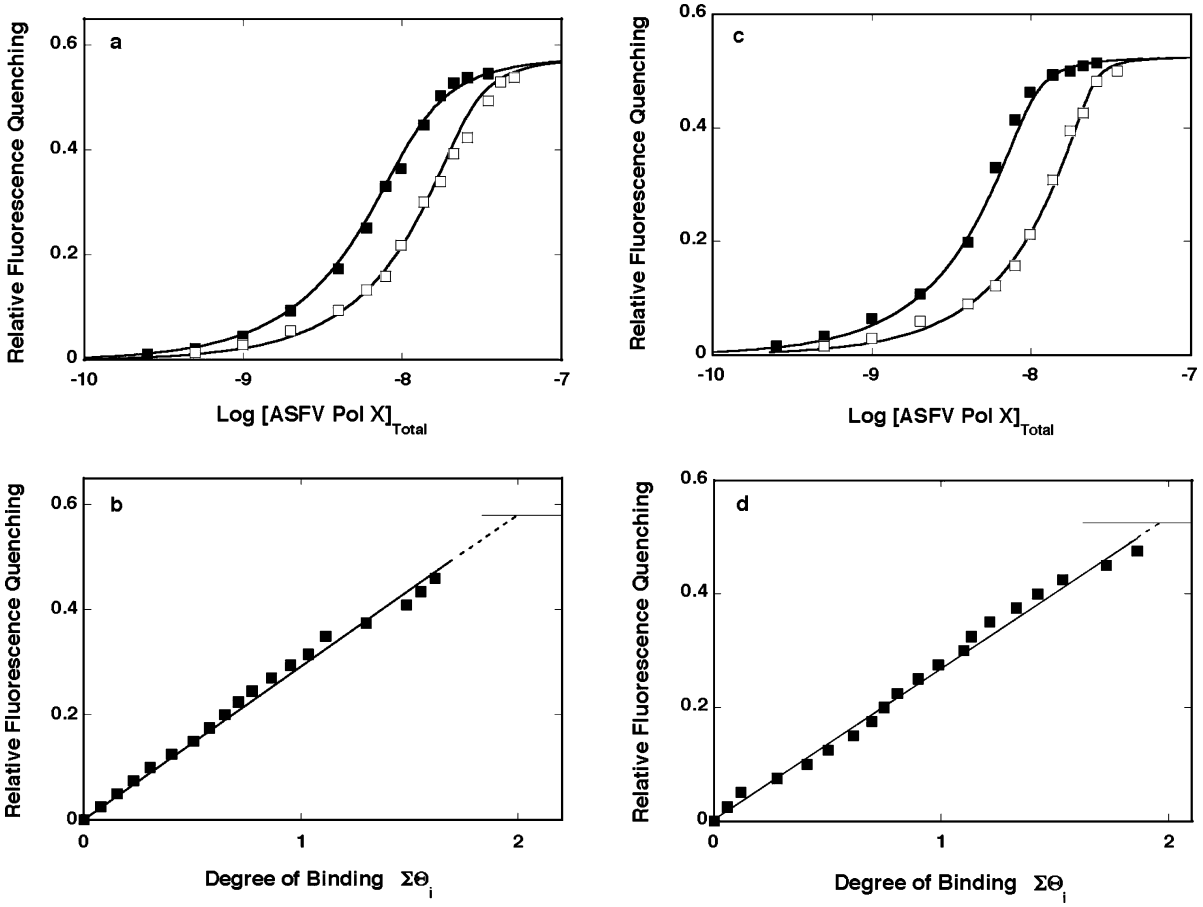

FIGURE 3: (a) Fluorescence titrations of a gapped DNA substrate with five nucleotides in the ssDNA gap (Figure 2, substrate A) with the ASFV pol X in buffer C (pH 7.0, 10 °C), containing 198 mM NaCl, and 1 mM $MgCl_2$, at two different concentrations of the nucleic acid, 5×10^{-9} M (■) and 1.2×10^{-8} M (□), respectively. The solid lines are the nonlinear least-squares fits of the experimental titration curves to the model of two distinct cooperative binding sites (eqs 4−6) using a single set of binding and spectroscopic parameters, $K_G = 6.5 \times 10^8$ M^{-1}, $K_D = 6.5 \times 10^8$ M^{-1}, $\sigma = 1$, $\Delta F_G = 0.29$, and $\Delta F_D = 0.29$ (see text for details). (b) The dependence of the observed relative fluorescence quenching, ΔF, upon the total average degree of binding, $\sum\Theta_i$, of the ASFV pol X on the DNA substrate with five nucleotide residues in the ssDNA gap. The values of $\sum\Theta_i$ have been obtained using the quantitative approach described in Materials and Methods. The solid line follows the experimental points and does not have a theoretical basis. The dashed line is an extrapolation of the plot to the maximum observed fluorescence quenching, ΔF_{max}, marked by horizontal solid line. (c) Fluorescence titrations of a gapped DNA substrate with two nucleotides in the ssDNA gap (Figure 2, substrate D) with the ASFV pol X in buffer C (pH 7.0, 10 °C), containing 198 mM NaCl and 1 mM $MgCl_2$, at two different concentrations of the nucleic acid, 5×10^{-9} M (■) and 1.2×10^{-8} M (□), respectively. The solid lines are the nonlinear least-squares fits of the experimental titration curves to the model of two distinct cooperative binding sites (eqs 4−6) using a single set of binding and spectroscopic parameters, $K_G = 6 \times 10^{10}$ M^{-1}, $K_D = 6.5 \times 10^8$ M^{-1}, $\sigma = 230$, $\Delta F_G = 0.263$, and $\Delta F_D = 0.263$ (see text for details). (d) The dependence of the observed relative fluorescence quenching, ΔF, upon the total average degree of binding, $\sum\Theta_i$, of the ASFV pol X on the DNA substrate with two nucleotides in the ssDNA gap. The values of $\sum\Theta_i$ have been obtained using the quantitative approach described in Materials and Methods. The solid line follows the experimental points and does not have a theoretical basis. The dashed line is an extrapolation of the plot to the maximum observed fluorescence quenching, ΔF_{max}, marked by the solid horizontal line.

average degree of binding, $\sum\Theta_i$, of the ASFV pol X on the considered DNA substrate. As previously observed (Figure 3b), the plot is, within experimental accuracy, linear. We could determined the value of the total average degree of binding up to $\sum\Theta_i \sim 1.9$. Very short extrapolation of $\sum\Theta_i$ to the maximum fluorescence quenching, $\Delta F_{max} = 0.53 \pm 0.04$, provides $\sum\Theta_i = 2 \pm 0.2$. Thus, at saturation, two ASFV pol X molecules bind to the gapped DNA substrate containing two nucleotides in the ssDNA gap, the same number of polymerase molecules as observed for the substrate with five nucleotides in the gap (Figure 3b). Analogous, quantitative studies have been performed with the entire series of the gapped DNA substrates, and the obtained maximum stoichiometries are included in Table 1. It is evident that the maximum stoichiometry of the ASFV pol X−gapped DNA complex does depend upon the size of the ssDNA gap (see Discussion).

Statistical Thermodynamic Model of ASFV Pol X−Gapped DNA Interactions. The data discussed below show that the binding of the ASFV pol X to the gapped DNA substrates with the ssDNA gap containing less than four nucleotides is characterized by a significantly higher affinity than the binding of the second ASFV pol X molecule (see below). This indicates that, analogously to the mammalian pol β, at a lower concentration of the enzyme, the ASFV pol X can form a high-affinity gap complex (*21*, *22*). Moreover, the enzyme can also associate with the dsDNA parts of the nucleic acid with significantly lower affinity than in the gap complex. At higher protein concentrations, two polymerase molecules are associated with the DNA substrate, each

Table 1: Thermodynamic and Spectroscopic Parameters for ASFV Pol X Binding to the Gapped-DNA Substrates, Differing in the Number of the Nucleotides in the ssDNA Gap (Figure 2), in Buffer C (pH 7.0, 10 °C) Containing 198 mM NaCl and 1 mM $MgCl_2$[a]

ssDNA gap (*N*)	maximum stoichiometry	K_G (M^{-1})	K_D (M^{-1})	σ	ΔF_G	ΔF_D	ΔF_{max}
1	2.0 ± 0.2	$(6.0 \pm 1.6) \times 10^{10}$	$(6.5 \pm 1.6) \times 10^{8}$	200 ± 60	0.53 ± 0.03	0.12 ± 0.03	0.65 ± 0.04
2	2.0 ± 0.2	$(6.0 \pm 1.6) \times 10^{10}$	$(6.5 \pm 1.6) \times 10^{8}$	230 ± 60	0.26 ± 0.03	0.26 ± 0.03	0.53 ± 0.04
3	2.3 ± 0.2	$(2.0 \pm 0.4) \times 10^{10}$	$(6.5 \pm 1.6) \times 10^{8}$	30 ± 10	0.55 ± 0.05	0.11 ± 0.03	0.66 ± 0.04
4	2.3 ± 0.2	$(1.3 \pm 0.3) \times 10^{9}$	$(6.5 \pm 1.6) \times 10^{8}$	2.8 ± 1	0.33 ± 0.03	0.32 ± 0.03	0.65 ± 0.03
5	2.0 ± 0.2	$(6.5 \pm 1.6) \times 10^{8}$	$(6.5 \pm 1.6) \times 10^{8}$	1.0 ± 0.3	0.29 ± 0.03	0.29 ± 0.03	0.58 ± 0.03

[a] The errors are standard deviations determined using 3−4 independent titration experiments. See text for details.

molecule associated with the dsDNA part of the gapped DNA substrate (*21*, *22*, *26*, *42*, *48*−*50*). The simplest partition function, Z_G, of the system, which describes such behavior, is defined by

$$Z_G = 1 + (K_G + K_D)P_F + \sigma K_D^{\,2} P_F^{\,2} \quad (4)$$

where K_G and K_D are intrinsic binding constants characterizing the formation of the high-affinity gap complex and the weak-affinity complex of the ASFV pol X with the dsDNA parts of the gapped DNA substrate, respectively. The quantity σ is the cooperative interactions parameter, which characterizes possible cooperative interactions between bound ASFV pol X molecules. The total average degree of binding, $\sum\Theta_i$, is then defined as

$$\sum\Theta_i = \frac{(K_G + K_D)P_F + 2\sigma K_D^{\,2} P_F^{\,2}}{Z_G} \quad (5)$$

The observed relative fluorescence quenching, ΔF, is described by

$$\Delta F = \frac{\Delta F_G K_G P_F + \Delta F_D K_D P_F + 2\Delta F_D \sigma K_D^{\,2} P_F^{\,2}}{Z_G} \quad (6)$$

where ΔF_G, and ΔF_D are the relative molar fluorescence quenchings of the DNA emission characterizing ASFV pol X binding in the high-affinity gap complex and the weak-affinity complex with the dsDNA (*21*, *22*, *26*).

There are five independent parameters ΔF_G, ΔF_D, K_G, K_D, and σ in eqs 4−6. This is a formidable number of parameters. However, some of them can be independently determined. Thus, because of the much higher affinity of the gap complex, the values of ΔF_G can be obtained from the plots of ΔF as a function of $\sum\Theta_i$, as depicted in Figures 3b and 3c, $\Delta F_G = d\Delta F/d(\sum\Theta_i)$. Moreover, the linear character of the plots in Figures 3b and 3c indicates that $\Delta F_G = \Delta F_D$ for these particular DNA substrates (Table 1). The value of ΔF_D can be determined from the maximum observed fluorescence quenching as $\Delta F_{max} = 2 \times \Delta F_D$. Nevertheless, there are still three binding parameters, K_G, K_D, and σ, which remain to be determined. The strategy of determining them is discussed below.

Intrinsic Affinities and Cooperativities of ASFV Pol X Binding to the Gapped DNA Substrates in the Presence of Magnesium. The solid lines in Figure 3a are nonlinear least-squares fits of the experimental titration curves to eqs 4−6 with three fitting parameters, which provide $K_G = (6.5 \pm 1.6) \times 10^8$ M^{-1}, $K_D = (6.5 \pm 1.6) \times 10^8$ M^{-1}, and $\sigma = 1$, for the gapped DNA substrate with 5 nucleotides in the ssDNA gap. The theoretical curves provide an excellent description of the experimental titration curves. Thus, the obtained data indicate that binding of each of the two ASFV pol X molecules to the DNA substrate containing five nucleotides in the ssDNA gap is characterized by virtually the same affinity, independent of the presumed nature of the formed complexes (see above). The profound meaning of these data is that they indicate that, with the substrate containing the ssDNA gap with five nucleotides, the ASFV pol X is not capable of forming the high-affinity gap complex to any detectable extent. Moreover, the cooperativity parameter value is $\sigma = 1$, indicating the lack of any cooperative interactions between the bound enzyme molecules. In other words, what is observed for this substrate is the independent binding of the two ASFV pol X molecules to two dsDNA parts of the nucleic acid. In addition, these results provide the intrinsic binding constant, K_D, for the independent binding of the ASFV pol X to the dsDNA parts of the gapped DNA substrate with the value of $(6.5 \pm 1.6) \times 10^8$ M^{-1}. Notice, because the binding process is independent, the value of K_D must be the same for all examined DNA substrates in the same solution conditions (see below).

Knowing the value of $K_D = (6.5 \pm 1.6) \times 10^8$ M^{-1}, we can address the binding to the gapped DNA substrates with fewer than five nucleotides in the ssDNA gap. In the case of the gapped DNA substrate with two nucleotides in the gap, the linear character of the plot in Figure 3d indicates that $\Delta F_G = \Delta F_D = 0.26 \pm 0.03$. This leaves three binding parameters, K_G, K_D, and σ, to be determined. However, unlike the case of the substrate with five nucleotides in the gap, the value of K_G cannot be obtained in direct fitting of the titration curves in Figure 3c. This is because the first ~50% of the titration curve is nearly stoichiometric, i.e., the concentration of the free pol X, P_F, constitutes an experimentally undetectable fraction of the total protein concentration, P_T, at low total polymerase concentrations (*26*). On the other hand, the value of K_G at 198 mM NaCl can be determined from the salt dependence of the intrinsic affinities of the enzyme discussed below, which provides $K_G = (6.0 \pm 1.6) \times 10^{10}$ M^{-1}. The solid lines in Figure 3c are nonlinear least-squares fits of the experimental isotherm to eqs 4−6, using the determined values of ΔF_G, ΔF_D, K_G, and K_D with a single fitting parameter, σ, which provide $\sigma = 230 \pm 60$. Analogous analyses have been performed for all examined gapped DNA substrates, with the obtained spectroscopic and binding parameters included in Table 1. Moreover, competition experiments with unmodified gapped DNA substrates, which contain adenosine in place of the fluorescein moiety, provide, within experimental accuracy, stoichiometries and binding parameters undistinguishable from the substrates containing fluorescein in the gap (data not shown) (*26*, *42*).

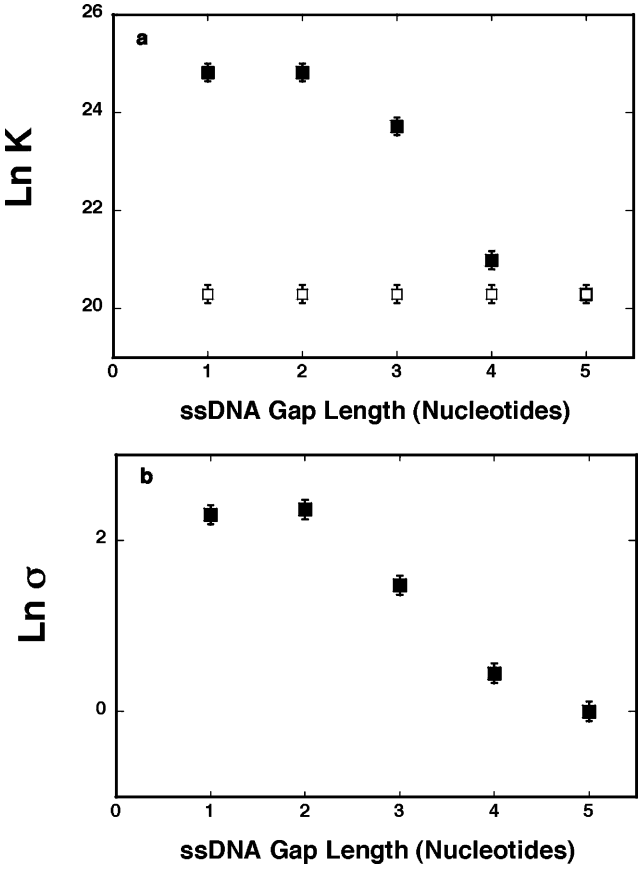

FIGURE 4: (a) The dependence of the intrinsic binding constant, K_G (■) and K_D (□), characterizing the formation of the gap complex and the binding to the dsDNA, respectively, upon the length of the ssDNA gap (nucleotides), in buffer C (pH 7.0, 10 °C), containing 198 mM NaCl and 1 mM $MgCl_2$. (b) The dependence of the cooperativity parameter, σ, characterizing cooperative interactions between bound ASFV pol X molecules, upon the length of the ssDNA gap (nucleotides), in buffer C (pH 7.0, 10 °C), containing 198 mM NaCl and 1 mM $MgCl_2$.

The dependence of the natural logarithm of the intrinsic binding constants, K_G and K_D, as a function of the length of the ssDNA gap (nucleotides) is shown in Figure 4a. Such a plot reflexes the relative free energy differences between the formed complexes with the gapped DNA substrate. For the ssDNA gap containing one and two nucleotide residues, the obtained value of the intrinsic binding constants, K_G, characterizing the formation of the gap complex, is a factor of $\sim$ 200 higher than the intrinsic binding constant, K_D, for the association with the dsDNA, which is the same for all DNA substrates (see above). For the ssDNA gap containing three nucleotides, the value of K_G is diminished by a factor of $\sim$3, from 6×10^{10} M^{-1} to 2×10^{10} M^{-1}. The dramatic drop in the value of K_G by a factor of $\sim$50 is observed for the gap containing four nucleotides. Finally, as pointed out above, when the ssDNA gap contains 5 nucleotides, pol X is not capable of forming the gap complex. The enzyme exclusively binds to two dsDNA, resulting in the same apparent values of K_G and K_D (see Discussion).

These changes in the intrinsic affinities, as a function of the length of the ssDNA gap, are paralleled by the changes in the cooperative interactions. Figure 4b shows the dependence of the natural logarithm of the cooperative interaction parameter, σ, as a function of the length of the gap. The substrates with the ssDNA gap containing one and two nucleotides have similar values of σ, i.e., approximately 200. For the gap with three and four nucleotides, the value of σ diminishes by an order of magnitude for each additional nucleotide, until it reaches the value of 1 for the substrate containing five nucleotides in the gap (see Discussion). Notice, the cooperative interactions were not detectable for the ASFV pol X binding to the ssDNA (*18*) (see Discussion).

Salt Effect on ASFV Pol X−Gapped DNA Interactions. To obtain further insight into the ASFV pol X interactions with the gapped DNA substrates, we examined the salt effect on the intrinsic affinities and cooperativity of the ASFV pol X binding to gapped DNA substrates. The experiments have been performed with the gapped DNA substrate with the ssDNA gap containing only two nucleotides (Figure 2, substrate D) and the gapped DNA substrate with the ssDNA gap containing five nucleotides (Figure 2, substrate A). Recall, the ASFV pol X is not capable of forming the gap complex when the ssDNA gap contains five nucleotides, while with the gapped DNA substrate having two nucleotides in the gap the polymerase can form the high-affinity gap complex (Table 1). Fluorescence titrations of the gapped DNA substrate, having the ssDNA gap containing five nucleotides, with the ASFV pol X in standard buffer, containing 1 mM $MgCl_2$ and different NaCl concentrations, are shown in Figure 5a. At higher concentrations of NaCl, the titration curves shift toward higher total protein concentrations, indicating a decreasing macroscopic affinity of the polymerase−nucleic acid complex. Quantitative analysis of the titration curves shown in Figure 5a, to extract binding and spectroscopic parameters, has been performed analogously, as described above.

The dependence of the logarithm of the binding constants, K_G and K_D, upon the logarithm of [NaCl] (log−log plot) is shown in Figure 5b (*51*, *52*). There are two important aspects of these data. First, at any salt concentration, the values of both binding constants are virtually identical and the value of the cooperativity parameter, σ, is 1 (Figure 5a). These results fully support the conclusion that the gap complex is not formed and independent and exclusive binding of the ASFV pol X to two dsDNA parts of the DNA substrate is observed (see above and Discussion). Second, both binding constants show virtually the same dependence upon the salt concentration. These data are also in excellent agreement with the independent and exclusive binding of two ASFV pol X molecules to two dsDNA parts. In other words, the same salt effect should be observed for the binding of the ASFV pol X to the dsDNA parts of any other gapped DNA substrates where the polymerase can form the gap complex (see below). The plots are linear in examined salt concentration ranges with the slope of the plots, $(\partial \log K_G)/(\partial \log [NaCl]) = (\partial \log K_D)/(\partial \log [NaCl]) = -1.4 \pm 0.3$, indicating that, in examined solution conditions, association of the polymerase with each of the dsDNA parts of the gapped DNA substrate is accompanied by the net release of $\sim$1.4 ions (*51*, *52*).

The situation is very different for the gapped DNA substrate with the ssDNA gap containing two nucleotides, where the ASFV pol X forms the high-affinity gap complex. Fluorescence titrations of the gapped DNA substrate, having the ssDNA gap containing two nucleotides, with the ASFV pol X are shown in Figure 5c. Quantitative analysis of the titration curves, shown in Figure 5c, has been performed

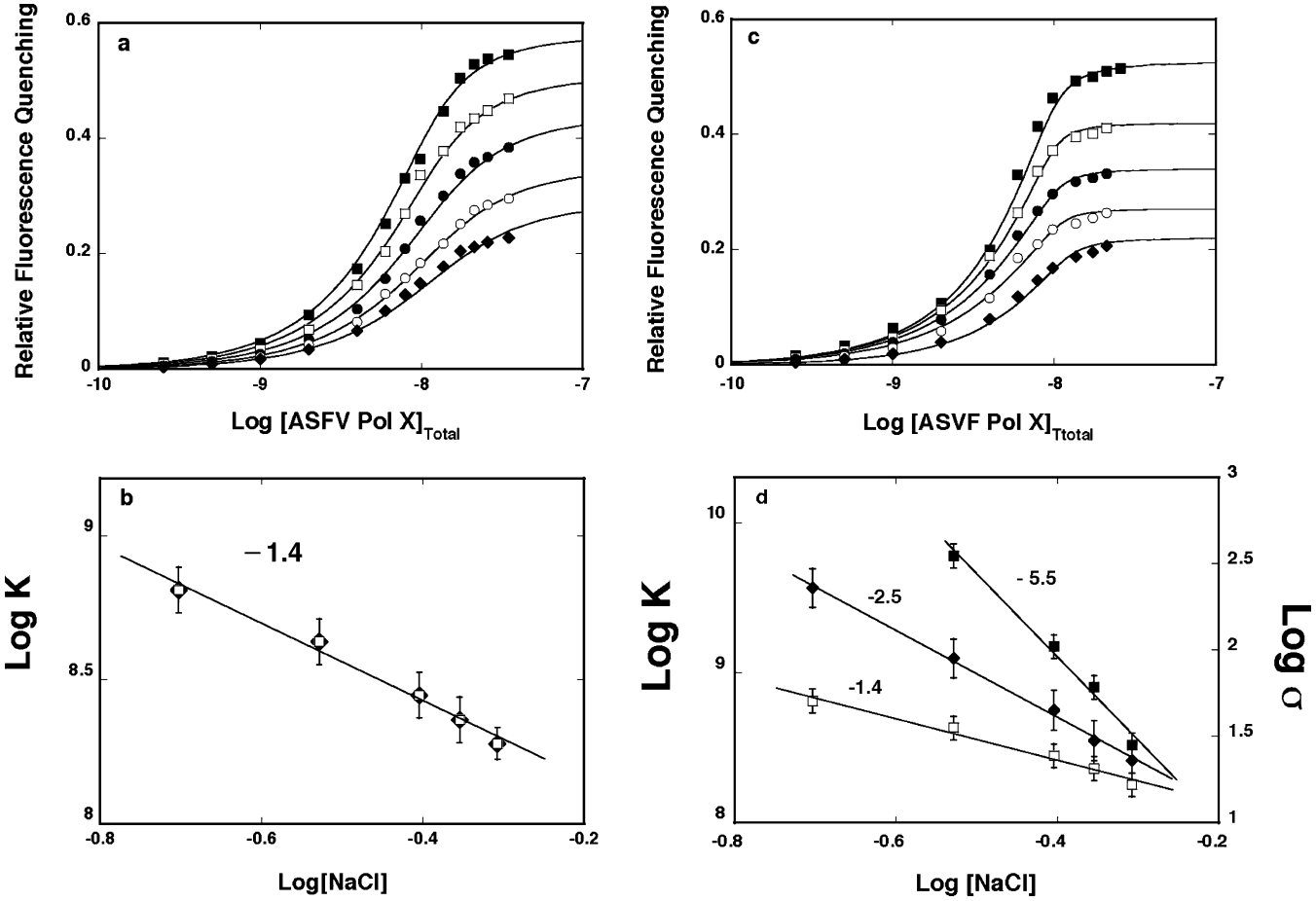

FIGURE 5: (a) Fluorescence titrations of the gapped DNA substrate with five nucleotides in the ssDNA gap (Figure 2, substrate A) with the ASFV pol X in buffer C (pH 7.0, 10 °C), containing 1 mM $MgCl_2$ and different NaCl concentrations: (■) 198 mM, (□) 296 mM, (●) 394 mM, (○) 443 mM, (◆) 493 mM. The solid lines are the nonlinear least-squares fits of the experimental titration curves to the model of two distinct cooperative binding sites (eqs 4−6), using $K_G = 6.5 \times 10^8$ M^{-1}, $K_D = 6.5 \times 10^8$ M^{-1}, $\sigma = 1$, $\Delta F_G = 0.29$, and $\Delta F_D = 0.29$ (■), $K_G = 4.3 \times 10^8$ M^{-1}, $K_D = 4.3 \times 10^8$ M^{-1}, $\sigma = 1$, $\Delta F_G = 0.26$, and $\Delta F_D = 0.26$ (□), $K_G = 2.8 \times 10^8$ M^{-1}, $K_D = 2.8 \times 10^8$ M^{-1}, $\sigma = 1$, $\Delta F_G = 0.24$, and $\Delta F_D = 0.20$ (●), $K_G = 2.3 \times 10^8$ M^{-1}, $K_D = 2.3 \times 10^8$ M^{-1}, $\sigma = 1$, $\Delta F_G = 0.20$, and $\Delta F_D = 0.15$ (○), $K_G = 1.8 \times 10^8$ M^{-1}, $K_D = 1.8 \times 10^8$ M^{-1}, $\sigma = 1$, $\Delta F_G = 0.18$, and $\Delta F_D = 0.11$ (◆). The concentrations of the DNA substrate are 5×10^{-9} M. (b) The dependence of the logarithm of the intrinsic binding constants, K_G (■) and K_D (□), upon the logarithm of NaCl concentration, for the gapped DNA substrate with five nucleotides in the ssDNA gap (Figure 2, substrate A), in buffer C (pH 7.0, 10 °C) containing 1 mM $MgCl_2$. The slopes of the plots are included in the panel. (c) Fluorescence titrations of the gapped DNA substrate with two nucleotides in the ssDNA gap (Figure 2, substrate D) with the ASFV pol X in buffer C (pH 7.0, 10 °C), containing 1 mM $MgCl_2$ and different NaCl concentrations: (■) 198 mM, (□) 296 mM, (●) 394 mM, (○) 443 mM, (◆) 493 mM. The solid lines are the nonlinear least-squares fits of the experimental titration curves to the model of two distinct cooperative binding sites (eqs 4−6), using $K_G = 6 \times 10^{10}$ M^{-1}, $K_D = 6.5 \times 10^8$ M^{-1}, $\sigma = 230$, $\Delta F_G = 0.263$, and $\Delta F_D = 0.263$ (■), $K_G = 6 \times 10^9$ M^{-1}, $K_D = 4.3 \times 10^8$ M^{-1}, $\sigma = 90$, $\Delta F_G = 0.263$, and $\Delta F_D = 0.21$ (□), $K_G = 2 \times 10^9$ M^{-1}, $K_D = 2.8 \times 10^8$ M^{-1}, $\sigma = 45$, $\Delta F_G = 0.263$, and $\Delta F_D = 0.17$ (●), $K_G = 8 \times 10^8$ M^{-1}, $K_D = 2.3 \times 10^8$ M^{-1}, $\sigma = 30$, $\Delta F_G = 0.263$, and $\Delta F_D = 0.135$ (○), $K_G = 3.3 \times 10^8$ M^{-1}, $K_D = 1.8 \times 10^8$ M^{-1}, $\sigma = 23$, $\Delta F_G = 0.11$, and $\Delta F_D = 0.11$ (◆). The concentrations of the DNA substrate are 5×10^{-9} M. (d) The dependence of the logarithm of the intrinsic binding constants, K_G (■), K_D (□), and cooperativity parameter, σ (◆), upon the logarithm of NaCl concentration, for the gapped DNA substrate with two nucleotides in the ssDNA gap (Figure 2, substrate D), in buffer C (pH 7.0, 10 °C), containing 1 mM $MgCl_2$. The slopes of the plots are included in the panel.

analogously, as described above, with the following differences. The values of K_D at a given salt concentration, i.e., the salt dependence of the intrinsic affinity of the ASFV pol X for the dsDNA parts of the DNA substrate, have been taken as the same as observed in the independent binding of the ASFV pol X to the dsDNA parts of the gapped DNA substrates containing the ssDNA gap with five nucleotides (see above). Also, for the titration at the lowest applied salt concentration (198 mM NaCl), where the initial ~50% of the titration curve is nearly stoichiometric, the value of K_G has been determined from the salt dependence of K_G, using four values of the same parameter obtained at higher salt concentrations, where the titrations curves are not stoichiometric (Figures 5c and 5d).

The dependence of the logarithm of the binding constants, K_G, upon the logarithm of [NaCl] (log−log plot) is shown in Figure 5d. For comparison, the log−log plot for the K_D is also included in Figure 5d. Unlike the behavior of the gapped DNA substrate with five nucleotides in the ssDNA gap, both plots dramatically differ in the values of their slopes. For the gap complex, the slope is $(\partial \log K_G)/(\partial \log [NaCl]) = -5.5 \pm 0.6$, indicating that the net release of 5−6 ions accompanies the formation of the gap complex (*51*, *52*). It should be stressed that the value of K_G at 198 mM NaCl is not used in determining the slope, $(\partial \log K_G)/(\partial \log [NaCl])$, of the plot in Figure 5d, but it is determined from this plot (see above). Thus, this value of K_G is not included in the log−log plot. It is evident that the net number of ions

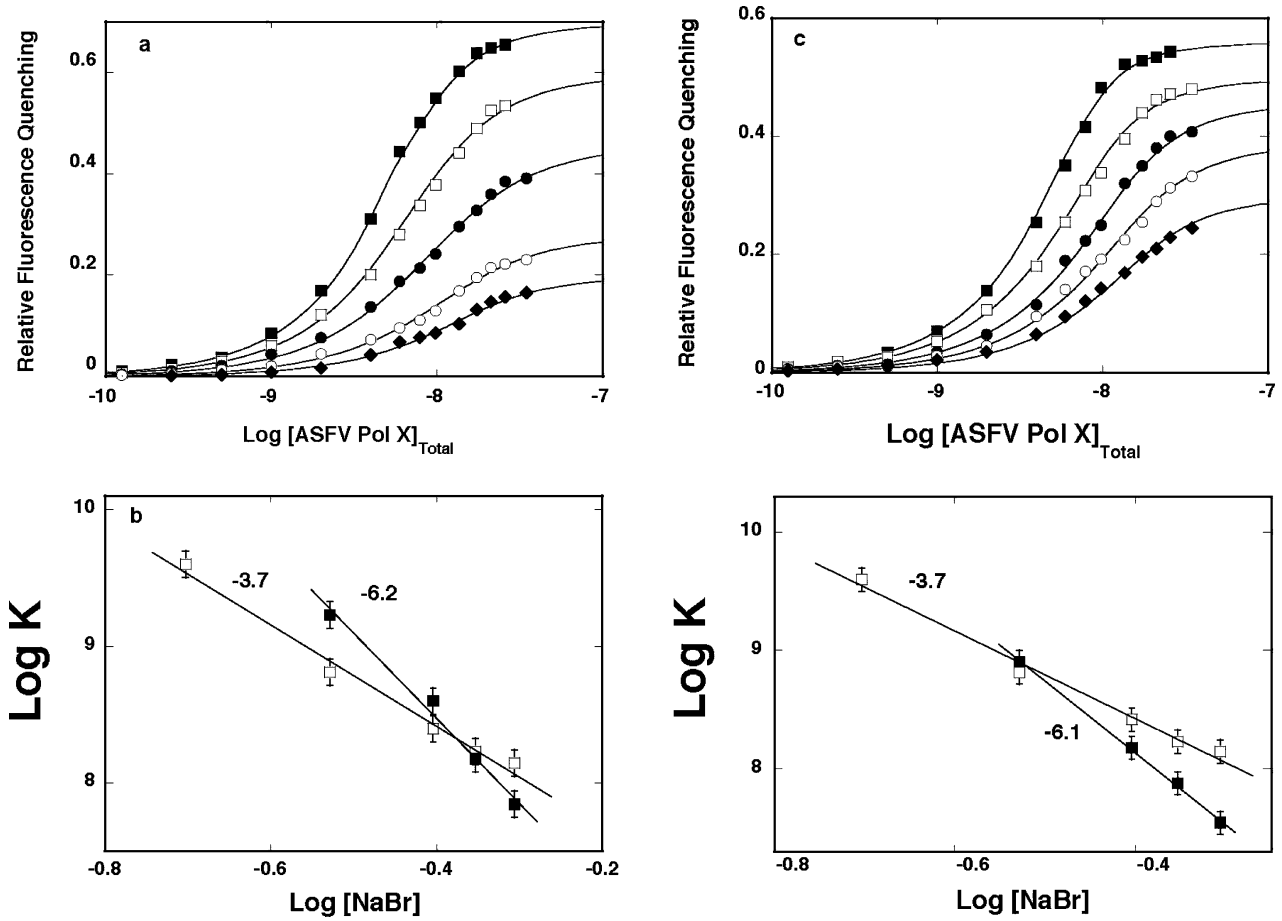

FIGURE 6: (a) Fluorescence titrations of the gapped DNA substrate with five nucleotides in the ssDNA gap (Figure 2, substrate A) with the ASFV pol X in buffer C (pH 7.0, 10 °C), containing 1 mM $MgCl_2$ and different NaBr concentrations: (■) 198 mM, (□) 296 mM, (●) 394 mM, (○) 443 mM, (◆) 493 mM. The solid lines are the nonlinear least-squares fits of the experimental titration curves to the model of two distinct cooperative binding sites (eqs 4−6) (see text for details), using $K_G = 4 \times 10^{10}$ M^{-1}, $K_D = 4 \times 10^9$ M^{-1}, $\sigma = 1$, $\Delta F_G = 0.41$, and $\Delta F_D = 0.35$ (■), $K_G = 1.7 \times 10^9$ M^{-1}, $K_D = 6.5 \times 10^8$ M^{-1}, $\sigma = 1$, $\Delta F_G = 0.33$, and $\Delta F_D = 0.30$ (□), $K_G = 4 \times 10^8$ M^{-1}, $K_D = 2.5 \times 10^8$ M^{-1}, $\sigma = 1$, $\Delta F_G = 0.26$, and $\Delta F_D = 0.23$ (●), $K_G = 1.5 \times 10^8$ M^{-1}, $K_D = 1.7 \times 10^8$ M^{-1}, $\sigma = 1$, $\Delta F_G = 0.18$, and $\Delta F_D = 0.14$ (○), $K_G = 8 \times 10^7$ M^{-1}, $K_D = 1.4 \times 10^8$ M^{-1}, $\sigma = 1$, $\Delta F_G = 0.12$, and $\Delta F_D = 0.10$ (◆). The concentrations of the DNA substrate are 5×10^{-9} M. (b) The dependence of the logarithm of the intrinsic binding constants, K_G (■) and K_D (□), upon the logarithm of NaBr concentration, for the gapped DNA substrate with five nucleotides in the ssDNA gap (Figure 2, substrate A), in buffer C (pH 7.0, 10 °C) containing 1 mM $MgCl_2$. The slopes of the plots are included in the panel. (c) Fluorescence titrations of the gapped DNA substrate with two nucleotides in the ssDNA gap (Figure 2, substrate D) with the ASFV pol X in buffer C (pH 7.0, 10 °C), containing 1 mM $MgCl_2$ and different NaCl concentrations: (■) 198 mM, (□) 296 mM, (●) 394 mM, (○) 443 mM, (◆) 493 mM. The solid lines are the nonlinear least-squares fits of the experimental titration curves to the model of two distinct cooperative binding sites (eqs 4−6), with $K_G = 2 \times 10^{10}$ M^{-1}, $K_D = 4 \times 10^9$ M^{-1}, $\sigma = 1$, $\Delta F_G = 0.37$, and $\Delta F_D = 0.28$ (■), $K_G = 7 \times 10^8$ M^{-1}, $K_D = 6.5 \times 10^8$ M^{-1}, $\sigma = 1$, $\Delta F_G = 0.35$, and $\Delta F_D = 0.25$ (□), $K_G = 1.5 \times 10^8$ M^{-1}, $K_D = 2.5 \times 10^8$ M^{-1}, $\sigma = 1$, $\Delta F_G = 0.31$, and $\Delta F_D = 0.23$ (●), $K_G = 7.5 \times 10^7$ M^{-1}, $K_D = 1.7 \times 10^8$ M^{-1}, $\sigma = 1$, $\Delta F_G = 0.27$, and $\Delta F_D = 0.195$ (○), $K_G = 3.5 \times 10^7$ M^{-1}, $K_D = 1.4 \times 10^8$ M^{-1}, $\sigma = 1$, $\Delta F_G = 0.24$, and $\Delta F_D = 0.15$ (◆). The concentrations of the DNA substrate are 5×10^{-9} M. (d) The dependence of the logarithm of the intrinsic binding constants, K_G (■), and K_D (□), upon the logarithm of NaBr concentration, for the gapped DNA substrate with two nucleotides in the ssDNA gap (Figure 2, substrate D), in buffer C (pH 7.0, 10 °C), containing 1 mM $MgCl_2$. The slopes of the plots are included in the panel.

released accompanying the formation of the gap complex is significantly larger than the net number of ions released upon binding of the polymerase exclusively to the dsDNA [$(\partial \log K_D)/(\partial \log [NaCl]) = -1.4 \pm 0.3$] (see Discussion). The log−log plot of the cooperativity parameter, σ, is also included in Figure 5d. The slope is $(\partial \log \sigma)/(\partial \log [NaCl]) = -2.5 \pm 0.5$, indicating that the net release of ∼2.5 ions accompanies the cooperative interactions between the bound pol X molecules (see Discussion).

Fluorescence titrations of the gapped DNA substrate, having the ssDNA gap containing five nucleotides, with the ASFV pol X in the standard buffer, containing 1 mM $MgCl_2$ and different NaBr concentrations, are shown in Figure 6a. Analogous fluorescence titrations of the gapped DNA substrate, with the ssDNA gap containing two nucleotides, are shown in Figure 6c. Quantitative analyses of the titration curves, shown in Figures 6a and 6c, have been performed analogously as described above, for titrations performed in the presence of NaCl. The replacement of chloride anions for bromide has a dramatic effect on the thermodynamic behavior of the system. Recall, in the presence of NaCl, the ASFV pol X is not capable of forming the gap complex when the ssDNA gap contains five nucleotides at any examined [NaCl] (Figure 4a). However, at a lower [NaBr], the values of K_G are significantly higher than the values of K_D for both gapped DNA substrates. Thus, in the presence of NaBr, the ASFV pol X can form the gap complex with the gapped DNA, which has the ssDNA gap containing five nucleotides

(see Discussion). Nevertheless, the cooperativity parameter value is $\sigma = 1$, indicating that binding of the enzyme to the dsDNA parts of the DNA substrates is still independent, as observed in the presence of NaCl. On the other hand, in the presence of NaCl or NaBr, the enzyme forms the gap complex when the ssDNA gap has only two nucleotides (Figure 6c). Nonetheless, the value of K_G, even at the lowest examined [NaBr] (198 mM), is only an order of magnitude larger than K_D, instead of 2 orders of magnitude difference, obtained at the same NaCl concentration (Figures 4a, 5a). Moreover, unlike the binding in the presence of NaCl, binding to the gapped DNA substrate, with the gap containing two nucleotides, in the presence of NaBr is characterized by $\sigma = 1$, at any examined [NaBr] (see Discussion).

The dependences of the logarithm of the binding constants, K_G and K_D, upon the logarithm of [NaBr] (log−log plot), for the gapped DNA substrate with five or two nucleotides in the ssDNA gap, are is shown in Figures 6b and 6d, respectively. In the case of the substrate with five nucleotides in the gap, the slopes of the plots are $(\partial \log K_G)/(\partial \log [NaBr]) = -6.2 \pm 0.8$ and $(\partial \log K_D)/(\partial \log [NaBr]) = -3.7 \pm 0.5$ (Figure 6b). For the gapped DNA substrate with two nucleotides in the gap, $(\partial \log K_G)/(\partial \log [NaBr]) = -6.1 \pm 0.8$ (Figure 6d). First, these data indicate that the gap complex is indeed formed with the substrate containing five nucleotides in the gap, which has the same thermodynamic response, to the increasing [NaBr], as the gap complex formed with the substrate containing the gap with two nucleotides. Second, both slopes are larger than the analogous parameters obtained in the presence of NaCl, indicating that anions participate in the ion release accompanying the formation of the gap complex and the ASFV pol X binding to the dsDNA parts of the gapped DNA substrates (see Discussion). It is interesting that the cooperativity parameter, σ, is independent of the [NaBr] concentration, while it is strongly dependent upon [NaCl] (Figures 7c and 5d). Such a profound difference, which depends on the type of anion in solution, indicates that anions are participating in ion release accompanying the cooperative interactions between bound pol X molecules (see Discussion) (*51*, *52*).

Role of Magnesium in ASFV Pol X−Gapped DNA Interactions. The experiments described so far have been performed in the presence of magnesium cations, which play a key role in the catalytic mechanisms of DNA polymerases (*9*, *15*, *17*, *53*). To assess the role of magnesium in the ASFV pol X interactions with the gapped DNA substrates, we examined the salt effect on intrinsic affinities and cooperativity of the pol X binding to the gapped DNA substrates in the absence of magnesium (*51*, *52*). Fluorescence titrations of the gapped DNA substrate, having the ssDNA gap containing five nucleotides, with pol X in the standard buffer, containing 0.1 mM EDTA and different NaCl concentrations, are shown in Figure 7a. Quantitative analysis of the titration curves, shown in Figure 7a, has been performed analogously, as discussed above, using the quantitative approach described in Materials and Methods (*26*, *30*−*33*, *36*−*45*). With the exception of the titration curve recorded at the lowest examined salt concentration (198 mM NaCl), the solid lines in Figure 7a are nonlinear least-squares fits with three binding parameters K_G, K_D, and σ as fitting parameters. For the titration performed at 198 mM NaCl, the value of K_G has been obtained from the salt dependence, based on the four values of K_G, determined at the remaining salt concentrations. Subsequently, this titration curve has been fitted with two binding parameters, K_D and σ (Figure 7a).

The results depicted in Figure 7a indicate a dramatic difference, as compared to the analogous data obtained in the presence of magnesium, and are analogous to the behavior observed in the presence of NaBr (see above). Thus, in the absence of magnesium, instead of independent and exclusive binding of the enzyme to two dsDNA parts of the gapped DNA substrate, the formation of the gap complex is clearly observed (Figure 7a). Although the difference between the affinities is not as pronounced as that observed in the presence of magnesium, the value of K_G is significantly larger, by approximately 1 order of magnitude, than K_D, particularly at lower salt concentrations, analogous to the behavior observed in the presence of NaBr (Figure 7a). The dependence of the logarithm of the intrinsic binding constants, K_G and K_D, upon the logarithm of [NaCl] (log−log plot), obtained in the absence of magnesium, is shown in Figure 7b. For the gap complex, the slope, $(\partial \log K_G)/(\partial \log [NaCl]) = -5.7 \pm 0.6$, indicating that the net release of 5−6 ions accompanies the formation of the gap complex, the same as observed in the presence of magnesium. On the other hand, the slope, $(\partial \log K_D)/(\partial \log [NaCl]) = -2.8 \pm 0.5$, is larger than that observed in the presence of Mg^{+2}. Nevertheless, it is approximately a factor of 2 smaller than determined for the gap complex. However, the cooperativity parameter value is $\sigma = 1$ at any examined salt concentration and indicates that the intrinsic binding constant, K_D, characterizes the independent binding of pol X to, exclusively, the dsDNA parts of the gapped DNA substrate.

Fluorescence titrations of the gapped DNA substrate, with the ssDNA gap having two nucleotides, with the ASFV pol X in the standard buffer, containing 0.1 mM EDTA and different NaCl concentrations, are shown in Figure 7c. Quantitative analysis of the titration curves, shown in Figure 7c, has been performed analogously as described for the analysis of titrations performed in the presence of magnesium. The dependence of the logarithm of the binding constants, K_G, on the logarithm of [NaCl] (log−log plot) is shown in Figure 7d (*51*, *52*). For comparison, the log−log plot for the K_D is also included in Figure 7d. In the absence of magnesium, the main aspects of this log−log plot are similar to the analogous plot obtained for the gapped DNA substrate with the ssDNA gap containing five nucleotides (Figure 7b). The slope, $(\partial \log K_G)/(\partial \log [NaCl]) = -5.1 \pm 0.6$, indicates that the net release of ~5 ions accompanies the formation of the gap complex as compared to net release of 2.8 ± 0.5 ions upon the exclusive binding to the dsDNA.

Binding of the ASFV pol X to gapped DNA substrates, in the absence of magnesium, has been performed for all examined gapped DNA substrates (Figure 2) (data not shown). The obtained interactions and spectroscopic parameters are included in Table 2. The dependence of the natural logarithm of the intrinsic binding constants, K_G and K_D, as a function of the length of the ssDNA gap is shown in Figure 8a. It is evident that, in the absence of magnesium, the value of K_G depends very little on the number of nucleotides in the ssDNA gap and remains higher than K_D. Thus, unlike the behavior of the enzyme in the presence of magnesium (Figure 4), the ASFV pol X forms the gap complex with the efficiency independent of the length of the ssDNA gap (see

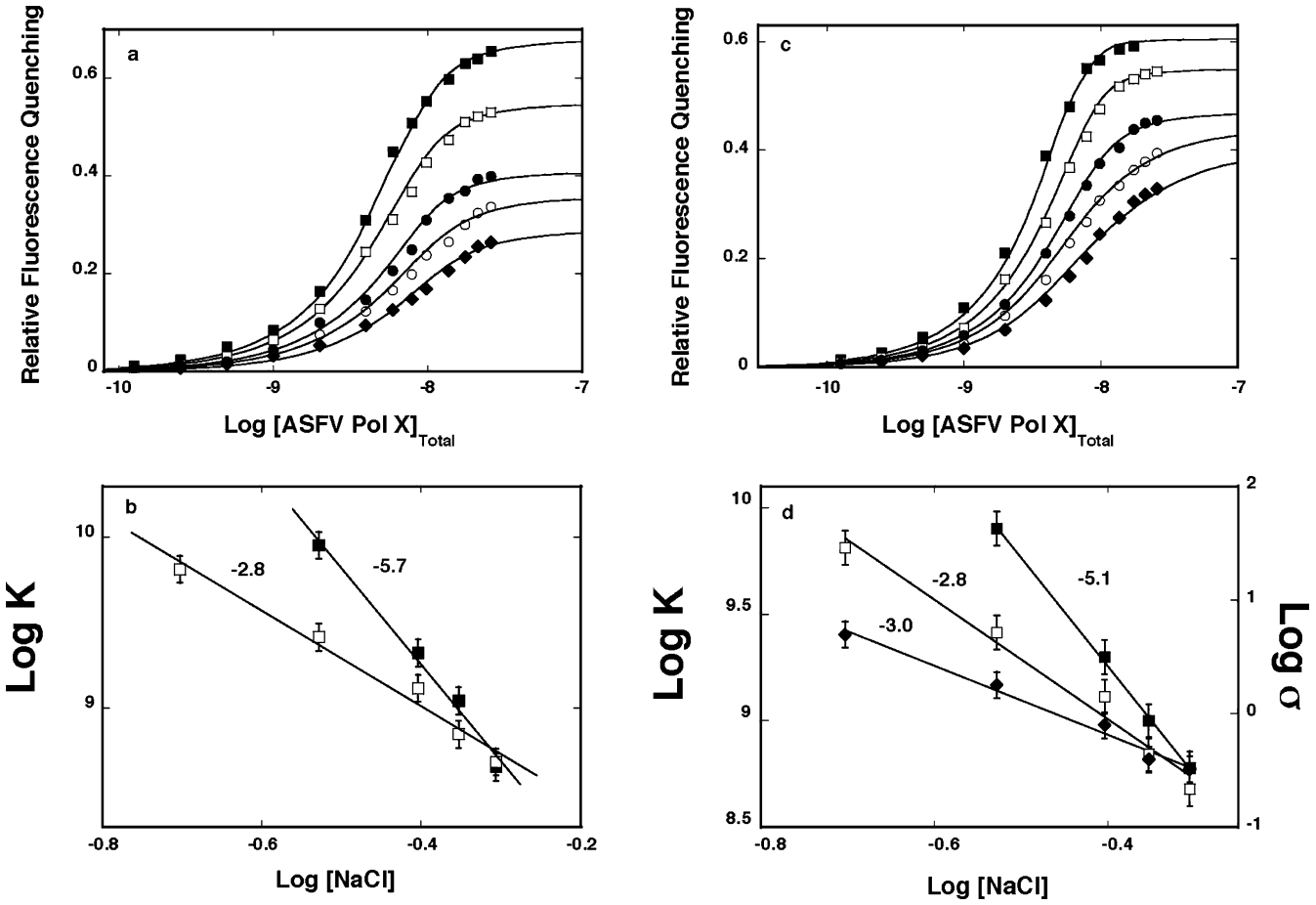

FIGURE 7: (a) Fluorescence titrations of the gapped DNA substrate with five nucleotides in the ssDNA gap (Figure 2, substrate A) with the ASFV pol X in buffer C (pH 7.0, 10 °C), containing 0.1 mM EDTA and different NaCl concentrations: (■) 198 mM, (□) 296 mM, (●) 394 mM, (○) 443 mM, (◆) 493 mM. The solid lines are the nonlinear least-squares fits of the experimental titration curves to the model of two distinct cooperative binding sites (eqs 4−6), with $K_G = 6 \times 10^{10}$ M^{-1}, $K_D = 6.5 \times 10^9$ M^{-1}, $\sigma = 1$, $\Delta F_G = 0.4$, and $\Delta F_D = 0.34$ (■), $K_G = 9 \times 10^9$ M^{-1}, $K_D = 2.6 \times 10^9$ M^{-1}, $\sigma = 1$, $\Delta F_G = 0.34$, and $\Delta F_D = 0.225$ (□), $K_G = 2.1 \times 10^9$ M^{-1}, $K_D = 1.3 \times 10^8$ M^{-1}, $\sigma = 1$, $\Delta F_G = 0.26$, and $\Delta F_D = 0.205$ (●), $K_G = 1.1 \times 10^9$ M^{-1}, $K_D = 7 \times 10^8$ M^{-1}, $\sigma = 1$, $\Delta F_G = 0.21$, and $\Delta F_D = 0.15$ (○), $K_G = 4.5 \times 10^8$ M^{-1}, $K_D = 4.8 \times 10^8$ M^{-1}, $\sigma = 1$, $\Delta F_G = 0.15$, and $\Delta F_D = 0.145$ (◆). The concentrations of the DNA substrate are 5×10^{-9} M. (b) The dependence of the logarithm of the intrinsic binding constants, K_G (■) and K_D (□), upon the logarithm of NaCl concentration for the gapped DNA substrate with five nucleotides in the ssDNA gap (Figure 2, substrate A), in buffer C (pH 7.0, 10 °C) containing 0.1 mM EDTA. The slopes of the plots are included in the panel. (c) Fluorescence titrations of the gapped DNA substrate with two nucleotides in the ssDNA gap (Figure 2, substrate D) with the ASFV pol X in buffer C (pH 7.0, 10 °C), containing 0.1 mM EDTA and different NaCl concentrations: (■) 198 mM, (□) 296 mM, (●) 394 mM, (○) 443 mM, (◆) 493 mM. The solid lines are the nonlinear least-squares fits of the experimental titration curves to the model of two distinct cooperative binding sites (eqs 4−6), with $K_G = 8 \times 10^{10}$ M^{-1}, $K_D = 6.5 \times 10^9$ M^{-1}, $\sigma = 5$, $\Delta F_G = 0.51$, and $\Delta F_D = 0.325$ (■), $K_G = 8 \times 10^9$ M^{-1}, $K_D = 2.6 \times 10^9$ M^{-1}, $\sigma = 1$, $\Delta F_G = 0.46$, and $\Delta F_D = 0.28$ (□), $K_G = 2 \times 10^9$ M^{-1}, $K_D = 1.3 \times 10^9$ M^{-1}, $\sigma = 0.8$, $\Delta F_G = 0.39$, and $\Delta F_D = 0.235$ (●), $K_G = 1 \times 10^9$ M^{-1}, $K_D = 7 \times 10^8$ M^{-1}, $\sigma = 0.4$, $\Delta F_G = 0.35$, and $\Delta F_D = 0.22$ (○), $K_G = 6 \times 10^8$ M^{-1}, $K_D = 4.8 \times 10^8$ M^{-1}, $\sigma = 0.33$, $\Delta F_G = 0.27$, and $\Delta F_D = 0.2$ (◆). The concentrations of the DNA substrate are 5×10^{-9} M. (d) The dependence of the logarithm of the intrinsic binding constants, K_G (■), K_D (□), and cooperativity parameter, σ (◆), upon the logarithm of NaCl concentration, for the gapped DNA substrate with two nucleotides in the ssDNA gap (Figure 2, substrate D), in buffer C (pH 7.0, 10 °C), containing 0.1 mM EDTA. The slopes of the plots are included in the panel.

Table 2: Thermodynamic and Spectroscopic Parameters for ASFV Pol X Binding to the Gapped-DNA Substrates, Which Differ in the Number of Nucleotide Residues in the ssDNA Gap (Figure 2), in Buffer C (pH 7.0, 10 °C) Containing 198 mM NaCl and 0.1 mM EDTA[a]

ssDNA gap (N)	maximum stoichiometry	K_G (M^{-1})	K_D (M^{-1})	σ	ΔF_G	ΔF_D	ΔF_{max}
1	2.0 ± 0.2	(8 ± 2) × 10^{10}	(6.5 ± 1.6) × 10^9	15 ± 5	0.48 ± 0.05	0.28 ± 0.03	0.56 ± 0.04
2	2.0 ± 0.2	(8 ± 2) × 10^{10}	(6.5 ± 1.6) × 10^9	5 ± 1.5	0.51 ± 0.05	0.30 ± 0.03	0.60 ± 0.04
3	2.1 ± 0.2	(8 ± 2) × 10^{10}	(6.5 ± 1.6) × 10^9	2.4 ± 0.8	0.35 ± 0.03	0.32 ± 0.03	0.64 ± 0.03
4	2.0 ± 0.2	(6 ± 1.4) × 10^{10}	(6.5 ± 1.6) × 10^9	1.5 ± 0.5	0.22 ± 0.03	0.29 ± 0.03	0.58 ± 0.03
5	2.1 ± 0.2	(6 ± 2) × 10^{10}	(6.5 ± 1.6) × 10^9	1.0 ± 0.3	0.40 ± 0.04	0.34 ± 0.03	0.68 ± 0.05

[a] The errors are standard deviations determined using 3−4 independent titration experiments. See text for details.

Discussion). Figure 8b shows the dependence of the natural logarithm of the cooperative interaction parameter, σ, as a function of the length of the gap. The values of σ are considerably lower, as compared to the same parameter observed in the presence of magnesium, indicating strongly diminished cooperative interactions (Figure 4b). Nevertheless, similar to the behavior observed in the presence of Mg^{+2}, the cooperative interaction parameter, σ, decreases

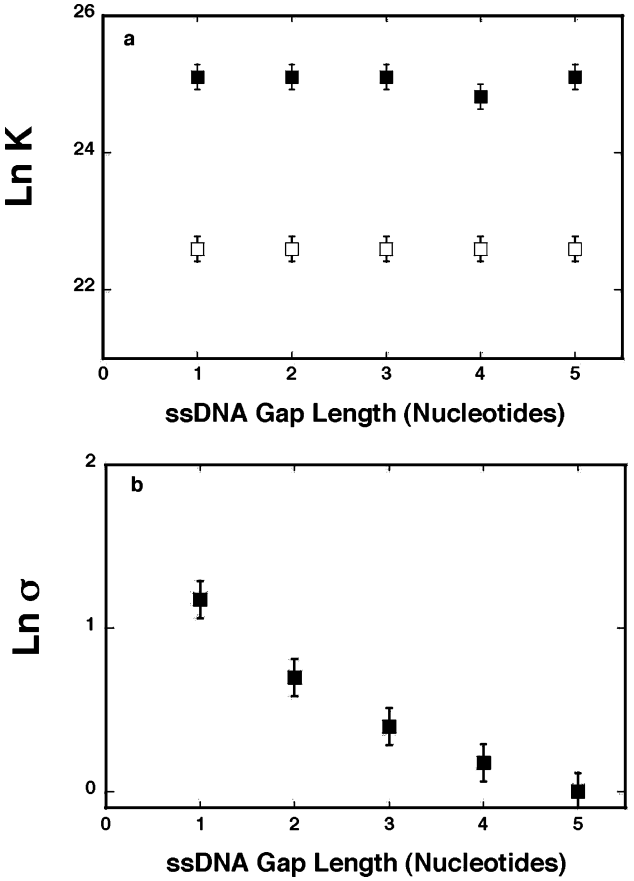

FIGURE 8: (a) The dependence of the intrinsic binding constant, K_G (■) and K_D (□), characterizing the formation of the gap complex and the binding to the dsDNA, respectively, upon the length of the ssDNA gap (nucleotides), in buffer C (pH 7.0, 10 °C), containing 198 mM NaCl and 1 mM $MgCl_2$. (b) The dependence of the cooperativity parameter, σ, characterizing cooperative interactions between bound ASFV pol X molecules, upon the length of the ssDNA gap (nucleotides), in buffer C (pH 7.0, 10 °C), containing 198 mM NaCl and 0.1 mM EDTA.

as the length of the ssDNA gap increases, reaching the value of 1 for the substrate containing 5 nucleotide residues (see Discussion). Also, the absence of magnesium very significantly affects the salt effect on the cooperative interactions between bound ASFV pol X molecules. The log−log plot of the cooperativity parameter, σ, obtained in the absence of magnesium, is included in Figure 7d. As the concentration of NaCl increases, σ strongly decreases, assuming values lower than 1 at [NaCl] > 300 mM. Thus, cooperative interactions become negative at a high salt concentration range (*55*). Nevertheless, within experimental accuracy, the plot is linear with the slope, $(\partial \log \sigma)/(\partial \log [\mathrm{NaCl}]) = -3.0 \pm 0.9$. Thus, in the absence of Mg^{+2} cations, the net number of ions released, as a result of cooperative interactions between bound ASFV pol X molecules, is very similar to the same parameter obtained in the presence of Mg^{+2} (see Discussion).

DISCUSSION

The Stoichiometry of ASFV Pol X−Gapped DNA Substrate Complexes Is Higher Than Predicted by the NMR Studies of the Enzyme. In spite of exceptionally simplified structure and catalytic activities, the recognition process of gapped DNA substrates by the ASFV pol X is a complex process, as indicated by the direct thermodynamic studies described in this work. Similar complex behavior was already evident in previous studies of the enzyme binding to seemingly simpler substrate, the ssDNA (*18*). A completely surprising feature of the examined interactions between the gapped DNA substrates and the ASFV pol X is the high maximum stoichiometry of the formed complexes. Thus, at saturation, two polymerase molecules are bound to the examined gapped DNAs (Table 1). Moreover, the observed maximum stoichiometry of two enzyme molecules bound to the gapped DNA is independent of the number of nucleotides in the ssDNA gap. This maximum stoichiometry, determined in equilibrium measurements, in solution, is dramatically different from the exclusively 1:1 maximum stoichiometry, suggested for the enzyme complexes with analogous gapped DNA substrates and based on NMR and gel shift studies (*16*, *17*). On the other hand, the observed maximum stoichiometry of the ASFV pol X−gapped DNA complex, as well as the nature of the binding process, can be understood in the context of the discovered functional heterogeneity of the total DNA-binding site of the enzyme, with respect to the interactions with the nucleic acid (*18*).

ASFV Pol X Forms Two Different Complexes with the Gapped DNA Substrates Differing Dramatically in Their Intrinsic Affinities. A peculiar aspect of the ASFV pol X binding to the examined gapped DNA substrates is the formation of two very different complexes, particularly, with the gapped DNA substrates containing the ssDNA gap with one or two nucleotides. This is unexpected because of the small size and the proposed rigid structure of the enzyme (*18*). Yet, when only a single molecule of the ASFV pol X is bound to the gapped DNA, the enzyme forms two different complexes with the nucleic acid. However, these two complexes differ by ~2 orders of magnitude in their intrinsic affinities (Table 1). First, such a large disparity in the affinities indicates that complexes of a very different nature are observed. Second, as the protein concentration increases, two ASFV pol X molecules, bound with low intrinsic affinity, replace the 1:1 complex with the high intrinsic affinity. This can occur only if the high-affinity complex has a larger site-size than the low-affinity complex, in other words, it is engaging a larger fragment of the nucleic acid than the low-affinity complex (*26*, *48*−*50*). This behavior is a consequence of the favorable entropy factor for the protein−nucleic acid complexes with the lower site-sizes, as compared to the complexes with larger site-sizes.

Analogous behavior has been previously observed for the binding of the mammalian pol β to the gapped DNA substrates and showed that it reflexes the formation of the catalytically active gap complex, which encompasses the total DNA-binding site of the enzyme and the binding to the dsDNA, where pol β uses only the DNA-binding subsite located on its 8 kDa domain (*55*). Therefore, on the basis of the obtained data, we assigned the high-affinity complex of the ASFV pol X as the gap complex, while the low-affinity complex reflexes the binding of the enzyme to the dsDNA parts of the gapped DNA substrates. The corresponding statistical thermodynamic model provides an excellent description of the complex binding process. Notice, a very strong indication of a very different nature of the formed complexes comes from the salt effect on their intrinsic affinities (Figures 5c and 5d). In the presence of magnesium,

the net number of ions released in the formation of the gap complex is ~5.5 while the analogous parameter for binding to the dsDNA is only ~1.4. These data strongly indicate that a significantly larger fragment of the nucleic acid is involved in the interaction with the protein in the gap complex, as compared to the binding to only the dsDNA part of the gapped DNA substrate. In other words, ASFV pol X is capable of forming a gap complex and engaging the two dsDNA parts of the gapped DNA substrate, or to associate with each dsDNA part of the substrate, using only one of its DNA-binding subsites.

In the Presence of Magnesium, ASFV Pol X Forms the Gap Complex with Strong Preference for the ssDNA Gaps with One or Two Nucleotides. Biochemical studies have clearly shown that the ASFV pol X has a catalytic preference for the gapped DNA substrates, with the ssDNA gap containing only one or two nucleotides during the DNA synthesis, i.e., in the presence of magnesium cations (*6*, *7*). In the case of the analogous mammalian pol β, the enzyme becomes processive on the gapped DNA substrates with fewer than six nucleotides in the gap. However, thermodynamic studies did not indicate any significant preference of the mammalian pol β for a particular size of the gap (*21*, *22*, *30*, *33*). In other words, the very dynamic structure of the mammalian pol β can adjust to the changing size of the gap, without an additional energy input. On the other hand, the preference for the ssDNA gaps containing three or four nucleotides has been observed for pol β in stopped-flow kinetic studies and attributed to the equilibria in the internal steps of the gap complex formation (*30*). Although the kinetic mechanism of the ASFV pol X binding to the gapped DNA substrates is still unknown, the obtained thermodynamic data already indicate that the behavior of the viral enzyme is different from the mammalian pol β, as depicted in Figure 4a. The ASFV pol X shows a strong preference for forming the gap complex, over the binding to the dsDNA. However, this happens only with gapped DNA substrates, which contain the ssDNA gap having one or two nucleotides. Therefore, these data provide direct evidence that the observed catalytic preference of the ASFV pol X for short ssDNA gaps during the DNA synthesis results from the strong energetic preference of the enzyme to form the gap complex with such DNA substrates (Figure 4a).

Nonetheless, our results indicate that, with the gapped DNA substrates containing the ssDNA with three nucleotides, the ASFV pol X will form the gap complex, although with a lower efficiency, as compared to the ssDNA with one or two nucleotides (Figure 4a). With four nucleotides in the gap, the enzyme will still form the gap complex, although the equilibrium is already strongly shifted toward the complex in which the polymerase is exclusively bound to the dsDNA. However, when the size of the ssDNA gap exceeds four nucleotides, pol X, unlike the mammalian pol β, loses is ability to form the gap complex. With the gapped DNA substrate containing the ssDNA gap with five nucleotides, the enzyme exclusively binds to the dsDNA parts of the substrate and the gap complex is undetectable (Figure 4a, Table 1). Moreover, the log−log plots for K_G and K_D have identical slopes, clearly indicating that in both complexes the enzyme interacts with a similar fragment of the nucleic acid, i.e., a single type of complex with the dsDNA parts of the gapped DNA substrate is formed. Therefore, unlike the mammalian pol β, the ASFV pol X, in the presence of magnesium, cannot energetically nor structurally adjust to the size of the ssDNA gap larger than two or three nucleotides. The obtained data indicates that the structure of the ASFV pol X is geared to specifically recognize the ssDNA gap containing only one or two nucleotides, with three nucleotides in the gap being the maximal threshold. Moreover, this specific recognition process already occurs in the ground state of the enzyme-gapped DNA complex, as built in the rigid structure of the polymerase, not in the subsequent steps in the association reaction. In turn, this specific structure is induced by magnesium and anion binding to the polymerase (see below).

In the Absence of Magnesium or the Presence of Sodium Bromide, ASFV Pol X Loses Its Selectivity for the ssDNA Gaps with One and Two Nucleotides. Direct Binding of Magnesium Cations to the Pol X Is a Major Factor in Inducing the Selectivity of the Polymerase for the Short ssDNA Gaps. The unusual aspect of the magnesium effect on the ASFV pol X interactions with the gapped DNA substrates is that fact that the removal of $MgCl_2$ from the solution completely abolishes the strong selectivity of the polymerase for the ssDNA gap containing one or two nucleotides (Figure 7a). This cannot be a simple ionic strength effect because the ionic strength of our solution conditions (~0.21) is affected very little by the removal of 1 mM magnesium chloride. This cannot be a simple competition between the protein and magnesium for the phosphate groups on the DNA, because such competition affects both the gap complex and the binding to the dsDNA parts of the gapped DNA substrate in the same direction, i.e., removal of magnesium reinforces the affinities of both complexes, although the effect on the dsDNA affinity is more pronounced. However, the affinity for the dsDNA is a part of the high affinity of the gap complex, as the enzyme interacts in both complexes with the double stranded conformation of the nucleic acid and removal of competing magnesium cations would increase, not decrease, the affinity difference between the gap complex and the dsDNA binding.

Rather, the observed effect indicates that direct and specific binding of Mg^{+2} cations to the ASFV pol X induces a specific conformational state of the enzyme molecule, in which the enzyme preferentially recognizes the ssDNA gaps with one or two nucleotides. In light of the data on the ASFV pol X binding to the ssDNA, previously obtained and the data discussed here, the binding of magnesium "stiffens" the conformation of the polymerase, making it well adjusted to form a high-affinity complex with the short ssDNA gaps with one and two nucleotides. On the other hand, in the absence of Mg^{+2}, the ASFV pol X has an increased affinity for the dsDNA and also a less "stiff" conformation. In such a more flexible conformational state, the enzyme, bound to one of the dsDNA parts of the gap substrate, can reach over a larger ssDNA gap and engage in interactions with the remaining dsDNA part, forming the gap complex, although with lower affinity. In other words, the specific structure of the ASFV pol X, which allows the enzyme to selectively recognize the ssDNA gaps containing one or two nucleotides, is controlled by specific magnesium binding to the enzyme. The fact that magnesium affects the values of the cooperativity parameter, σ, which characterizes cooperative interactions between the bound ASFV pol X molecules, by more than an order of

magnitude further supports the conclusion that Mg^{+2} cations bind directly to the enzyme (Figures 5d and 6d).

It should be pointed out that increasing the salt concentration in solution also weakens the preference of the ASFV pol X to form the gap complex over binding to the dsDNA, even for the gapped DNA substrates with two nucleotides. At [NaCl] approaching 0.5 M, the intrinsic affinity of the gap complex is virtually the same as the intrinsic affinity for the dsDNA (Figures 5c, 5d, 6c, and 6d). However, in this case, the nature of the observed diminishing selectivity is different from the effect exerted by magnesium. Both the affinity of the enzyme to form the gap complex and the affinity for the dsDNA become weaker with the increasing salt concentration. Because, in the gap complex, the enzyme engages twice as long a fragment of the dsDNA, in interactions with both DNA-binding subsites of the total DNA-binding site, the sensitivity of the gap complex to the increasing salt concentration in solution is approximately twice as large as observed for the independent binding to each of the dsDNA parts of the gapped DNA. Notice, in the presence of magnesium, in the case of the gapped DNA substrate with two nucleotides in the gap, the slope of the log−log plot for the intrinsic affinity of the polymerase in gap complex is $(\partial \log K_G)/(\partial \log [NaCl]) = -5.5 \pm 0.6$, while the slope of the log−log plot for the polymerase binding exclusively to the dsDNA is $(\partial \log K_D)/(\partial \log [NaCl]) = -1.4 \pm 0.3$, more than 2-fold lower than obtained for the gap complex. However, these values were obtained in the background of competing magnesium and sodium cations for the nucleic acid (*51*, *52*). In the absence of magnesium, where this competition is eliminated, $(\partial \log K_G)/(\partial \log [NaCl]) = -5.1 \pm 0.6$ and $(\partial \log K_D)/(\partial \log [NaCl]) = -2.8 \pm 0.5$, which is, within experimental accuracy, significantly closer to the expected difference by a factor of 2 between the two parameters. Therefore, what is observed, as a result of the increasing salt concentration, is not the diminished selectivity for the formation of the gap complex, over the affinity for the dsDNA, but vanishing affinities of both types of the formed complexes by the ASFV pol X with the gapped DNA substrate, with the affinity of the gap complex decreasing faster with the increasing salt concentration.

The effect of NaBr indicates additional complexity of the system. In spite of the presence of magnesium, replacement of chloride by the bromide anion also eliminates the selectivity of the enzyme for the ssDNA gaps with one or two nucleotides. Bromide anions are known to bind significantly stronger to anion binding sites of proteins than chloride (*56*). However, the observed effect is not a simple competition between the nucleic acid and the anions, in solution, for the protein. Thus, although the affinity of the gap complex is diminished, the affinity of the protein for the dsDNA is, in fact, increased in the presence of bromide. Moreover, the presence of bromide anions eliminates the cooperativity between bound protein molecules. Notice, increasing NaCl concentration, i.e., increasing saturation of anion binding sites, strongly decreases the values of the cooperative interaction parameter, σ, although σ does not approach 1 even at the highest [NaCl] examined, while in the presence of bromide anions, the cooperative interaction parameter value is $\sigma = 1$ at any [NaBr]. These data indicate that direct binding of anions to the protein is observed. Thus, in addition to magnesium, binding of anions to the ASFV pol X controls the orientation of the enzyme in the complex with the nucleic acid, the flexibility of the polymerase structure, and the ability of the enzyme to adjust to the changing size of the ssDNA gap. Moreover, the anion effect is opposite to the effect exerted by magnesium cations.

In the Presence of Magnesium, ASFV Pol X Binds to Gapped DNA Substrates with Significant Positive Cooperative Interactions between Bound Enzyme Molecules with the Cooperative Interactions Increasing with the Decreasing Size of the ssDNA Gap. A puzzling aspect of the ASFV pol X binding to the gapped DNA substrates, with fewer than four nucleotides in the ssDNA gap, is the presence of significant positive cooperative interactions between the ASFV pol X molecules associated with the dsDNA. The interactions are strongly increasing with the decreasing number of the nucleotides in the ssDNA gap, indicating that, to be effective, cooperative interactions require a close contact between the enzyme molecules. Moreover, cooperative interactions are particularly pronounced in the presence of magnesium, while in the absence of Mg^{+2}, they are diminished by an order of magnitude. On the other hand, the ASFV pol X binds to the ssDNA without any significant cooperative interactions (*18*). Such a dramatic difference in the nature of the binding processes of the ASFV pol X to two different conformations of the nucleic acid indicates that the enzyme must be in a very different orientation when bound to the dsDNA, as compared to its orientation in the complex formed with the ssDNA. Our laboratory is currently addressing this issue.

Significant positive cooperative interactions have been previously observed for the analogous mammalian pol β, but only in the pol β binding to the dsDNA and only in the presence of magnesium (*55*). This correspondence suggests a similar role of the positive cooperative interactions in the functioning of both enzymes, belonging to the same polymerase X family. However, the similarity ends here. While cooperative interactions of pol β strongly increase with the increase of salt concentration in solution, the cooperative interactions between the ASFV pol X molecules strongly decrease with the increasing concentration of NaCl, becoming negative in the absence of magnesium at high [NaCl], indicating different forces and/or mechanisms involved in forming the cooperative contacts between pol X and pol β. While the increased cooperative interactions compensate for the diminished intrinsic affinity of pol β for the dsDNA at higher salt concentrations, such compensation is absent in the ASFV pol X binding to the dsDNA. On the other hand, the affinity of the ASFV pol X for the dsDNA is ~4 orders of magnitude higher than the affinity of pol β for the same nucleic acid conformation in similar solution conditions, making such a compensation not necessary for the activities of the ASFV pol X (*55*).

Model of the ASFV Pol X Binding to Gapped DNA Substrates. A plausible model of the ASFV pol X binding to the gapped DNA substrates, based on the results obtained in this work, is depicted in Figure 9. The total DNA-binding site of the ASFV pol X has two distinct DNA-binding subsites, the proper DNA-binding site and the auxiliary DNA-binding area, which strongly differ in their DNA affinities (*18*, *39*, *40*). The total DNA-binding site occludes 16 ± 2 nucleotides, comparable in length to examined gapped DNA substrates (Figure 2). At a low protein concentration, the polymerase can bind the dsDNA part of

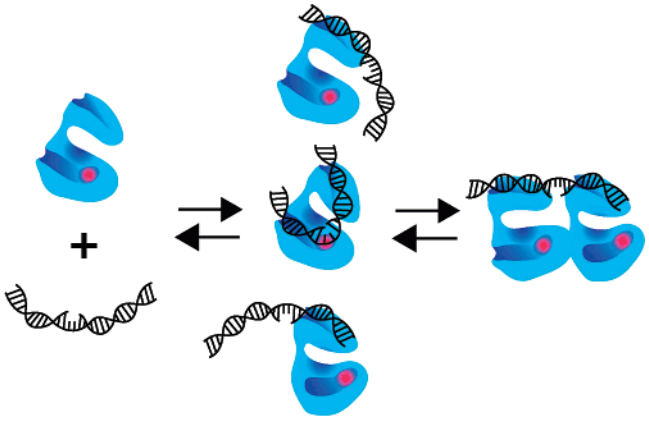

FIGURE 9: Model of the ASFV pol X binding to the gapped DNA substrate containing fewer than one or two nucleotides in the ssDNA gap, as a function of the enzyme concentration, based on the results obtained in this work. The total DNA-binding site of the ASFV pol X has two distinct DNA-binding subsites, the proper DNA-binding site and the auxiliary DNA-binding area, which strongly differ in their DNA affinities. At low protein concentration, the polymerase can bind the dsDNA of a gapped DNA substrate, using only one of its DNA-binding subsites. However, it can also engage both its DNA-binding areas, i.e., its total DNA-binding site, in interactions with both dsDNA parts of the gapped DNA substrate, forming the gap complex. However, as the protein concentration increases, the enzyme, bound using the total DNA-binding site, is forced to bind only to the dsDNA part of the gapped DNA substrate, which has a lower site-size. This transition is additionally reinforced by the strong positive cooperative interactions between bound ASFV pol X molecules. At a high ASFV pol X concentration, the complex with two pol X molecules bound to the gapped DNA substrate dominates the distribution of the formed complexes.

a gapped DNA substrate, using only its proper DNA-binding subsite (*39*, *40*). However, the enzyme can also engage both its DNA-binding subsites, i.e., its total DNA-binding site, in interactions with both dsDNA parts of the gapped DNA substrate, as long as the ssDNA gap is only one or two nucleotides long, leading to the formation of the gap complex, as depicted in Figure 9. Because both DNA-binding subsites are bound to the nucleic acid, the complex is characterized by a much higher affinity ($K_G \approx 10^{10}-10^{11}$ M^{-1}) as compared to the ASFV pol X binding to the dsDNA ($K_D = 10^8-10^9$ M^{-1}), using only a single DNA-binding subsite. However, as the protein concentration increases, the enzyme, initially bound using the total DNA-binding site, is forced to bind only to the dsDNA part of the gapped DNA substrate, presumably using only its proper DNA-binding subsite, which has a site-size of 7 ± 1 nucleotides (*18*). At a high ASFV pol X concentration, the complex with two ASFV pol X molecules bound to the gapped DNA substrate dominates the distribution of the formed complexes.

Additional Functional Implications. The remaining question is: what is the possible role of the discovered strong cooperative interactions in the ASFV pol X−dsDNA association in the recognition of the gapped DNA in the context of overwhelming dsDNA conformation? Previously, we proposed a model for the role of cooperative binding to the dsDNA in recognition of a damaged gapped DNA by pol β (*55*). The same model seems to apply to the analogous viral enzyme. The ASFV pol X cooperatively binds to the dsDNA, exclusively using one of its DNA-binding subsites. Cooperative interactions prevent the enzyme from dissociating from the nucleic acid. Instead of a single complex, a protein cluster is formed that allows the enzyme to examine longer patches of the dsDNA. This takes place only until the damaged DNA, i.e., the ssDNA gap, is encountered. Due to the high affinity, the enzyme forms a gap complex and changes its orientation on the DNA. In other words, the polymerase molecule, encountering the gap, breaks its ties with the protein cluster on the dsDNA upon forming the high-affinity gap complex. The enzyme, now free from interactions with the remaining ASFV pol X molecules bound to the dsDNA, engages the total DNA-binding site in interactions with the nucleic acid in a productive gap complex and may initiate catalytic steps (*55*).

Cooperative interactions, magnesium cations, and anions can also play a role in the selectivity of the ssDNA gap, which is catalytically active (*55*). Notice, the affinity of the gap complex is only significantly higher in the case of the gaps with one or two nucleotides, only in the presence of magnesium, and with chloride as the dominant monovalent anion. Therefore, only with such short gaps will there be enough of the free energy to break the cooperative contacts with the polymerase molecules bound to the dsDNA. In the case of gaps with four nucleotides, the affinity of the gap complex is much weaker and the cooperative interactions prevent the enzyme from efficiently forming the gap complex as discussed above. Changes in the concentration of Mg^{+2} cations around the DNA, or anions or the type of anion around the enzyme, provide additional and most probably entangled controls of the gap selectivity, superimposed on the cooperative interactions.

Our studies point also to an important caveat. As we have shown here for the ASFV pol X and previously for rat and human pol β, the interactions of these enzymes with their DNA substrates are significantly more complex than a simple formation of a single type of complex with the ssDNA, or exclusively a gap complex with the gapped DNA substrates. If it is assumed that only the activity of a specific complex, i.e., the gap complex, is observed, then the obtained kinetic and thermodynamic parameters from such studies are, at best, some mixture of catalytic activities of different complexes that overlap with an intricate web of multiple protein−protein, protein−ion, and protein−DNA interactions. The assumed reaction mechanisms and obtained kinetic and/or thermodynamic parameters, without elucidating and taking into account the entire complexity of the system, have more of a character of only plausible mechanisms and fitting constants than true mechanism and true physical constants that describe the examined system.

ACKNOWLEDGMENT

We thank Mrs. Gloria Bellard for reading the manuscript.

REFERENCES

1. Dixon, L. K., Abrams, C. C., Bowick, G., Goatley, L. C., Kay-Jackson, P. C., Chapman, D., Liverani, E., Nix, R., Silk, R., and Zhang, F. (2004) African Swine Fever Virus Proteins Involved In Evading Host Defense Systems, *Vet. Immunol. Immunopathol. 100*, 117−134.
2. Jouvnet, N., and Wileman, T. (2005) African Swine Fever Virus Infection Disrupts Centrosome Assembly and Function, *J. Gen. Virol. 86*, 589−594.
3. Takamatsu, H., Denyer, M. S., Oura, C., Childerstone, A., Andersen, J. K., Pullen, L., and Parkhouse, R. M. E. (1999)

African Swine Fever Virus: a B Cell-Mitogenic Virus *in vitro* and *in vivo*, *J. Gen. Virol. 208*, 249−278.
4. Yanez, R. J., Rodriguez, J. M., Nogal, M. L., Yuste, L., Enriquez, C., Rodriguez, J. F., and Vinuela, E. (1995) Analysis of the Complete Nucleotide Sequence of African Swine Fever Virus, *Virology 208*, 249−278.
5. Rubio, D., Alejo, A., Rodriguez, I., and Salas, M. L. (2003) Polyprotein Processing Protease of African Swine Fever Virus Purification and Biochemical Characterization *J. Virol. 77*, 4444−4448.
6. Oliveros, M., Yanez, R. R., Salas, M. L., Slas, J., Vinuela, E., and Blanco, L. (1997) Characterization of an African Fever Virus 20-kDa DNA Polymerase Involved in DNA Repair, *J. Biol. Chem. 272*, 30899−30910.
7. Garcia-Escudero, R., Garcia-Diaz, M., Salas, M. L., Blanco, L., and Salas, J. (2003) DNA Polymerase X of African Fever Virus: Insertion Fidelity on Gapped DNA substrates and AP lyase Activity Support a Role in Base Excision Repair of Viral DNA *J. Mol. Biol. 326*, 1403−1412.
8. Knopf, C. W. (1998) Evolution of Viral DNA-Dependent DNA Polymerases, *Virus Genes 16*, 47−58.
9. Hubscher, U., Nasheuer, H.-P., and Syvaoja, J. E. (2000) Eukaryotic DNA Polymerases, a Growing Family, *Trends Biochem. Sci. 25*, 143−147.
10. Matsumoto, Y., Kim, K., Katz, D. S., and Feng, J. A. (1998) Catalytic Center of DNA Polymerase β For Excision of Deoxyribose Phosphate Groups, *Biochemistry 37*, 6456−6464.
11. Masumoto, Y., and Kim, K. (1995) Excision of Deoxyribose Phosphate Residues by DNA Polymerase β During DNA Repair, *Science 269*, 699−702.
12. Sweasy, J. B. (2003) Fidelity Mechanisms of DNA Polymerase β, *Prog. Nucleic Acid Res. 73*, 137−168.
13. Budd, M. E., and Campbell, J. L. (1997) The Roles of the Eucaryotic DNA Polymerases in DNA Repair Synthesis, *Mutat. Res. 384*, 157−167.
14. Friedberg, E. C., Walker, G. C., and Siede, W. (1995) *DNA Repair and Mutagenesis*, pp 317−365, ASM Press, Washington, DC.
15. Maciejewski, M., Shin, R., Pan, B., Marintchev, A., Denninger, A., Mullen, M. A., Chen, K., Gryk, M. R., and Mullen, G. P. (2001) Solution Structure of a Viral DNA Repair Polymerase, *Nat. Struct. Biol. 8*, 936−941.
16. Showalter, A. K., Byeon, I.-J., Su, M.-I., and Tsai, M.-D. (2003) Solution Structure of a Viral DNA Polymerase X and Evidence for Mutagenic Function, *Nat. Struct. Biol. 8*, 942−946.
17. Showalter, A. K., and Tsai, M.-D. (2001) A DNA Polymerase With Specificity for Five Base Pairs, *J. Am. Chem. Soc. 123*, 1776−1777.
18. Jezewska, M. J., Marcinowicz, A., Lucius, A. L., and Bujalowski, W. (2006) DNA Polymerase X from African Swine Fever Virus Quantitative Analysis of the Enzyme - ssDNA Interactions and the Functional Structure of the Complex, *J. Mol. Biol. 356*, 121−141.
19. Rajendran, S., Jezewska, M. J., and Bujalowski, W. (1998) Human DNA polymerase β Recognizes Single-Stranded DNA Using Two Different Binding Modes, *J. Biol. Chem. 273*, 31021−31031.
20. Jezewska, M. J., Rajendran, S., and Bujalowski, W. (1998) Transition Between Different Binding Modes In Rat DNA Polymerase β - ssDNA Complexes, *J. Mol. Biol. 284*, 1113−1131.
21. Rajendran, S., Jezewska, M. J., and Bujalowski, W. (2001) Recognition of Template-Primer and Gapped DNA Substrates by Human DNA Polymerase β, *J. Mol. Biol. 308*, 477−500.
22. Jezewska, M. J., Rajendran, S., and Bujalowski, W. (2001) Energetics and Specificity of Rat DNA Polymerase β Interactions With Template-Primer and Gapped DNA substrates, *J. Biol. Chem. 276*, 16123−16136.
23. Jezewska, M. J., Rajendran, S., and Bujalowski, W. (2001) Interactions of the 8-kDa Domain of Rat DNA Polymerase β With ssDNA, *Biochemistry 40*, 3295−3307.
24. Jezewska, M. J., Galletto, R., and Bujalowski, W. (2003) Tertiary Conformation of the Template-Primer and Gapped DNA Substrates in Complexes With Rat Polymerase β Fluorescence Energy Transfer Studies Using the Multiple Donor-Acceptor Approach, *Biochemistry 42*, 11864−11878.
25. Galletto, R., Jezewska, M. J., and Bujalowski, W. (2005) Kinetic Mechanism of Rat Polymerase β - dsDNA Interactions Fluorescence Stopped-Flow Analysis of the Cooperative Ligand Binding to a Two-Site One-Dimensional Lattice, *Biochemistry 44*, 1251−1267.
26. Bujalowski, W. (2006) Thermodynamic and Kinetic Methods of Analyses of Protein − Nucleic Acid Interactions From Simpler to More Complex Systems, *Chem. Rev. 106*, 556−606.
27. Washington, M. T., Wolfle, W. T., Spratt, T. S., Prakash, L., and Prakash, S. (2003) Yeast DNA Polymerase η Makes Functional Contacts With the DNA Minor Groove Only At the Incoming Nucleotide Triphosphates, *Proc. Natl. Acad. Sci. U.S.A. 100*, 5113−5118.
28. Trinacao, J., Johnson, R. E., Wolfle, W. T., Escalante, C. R., Prakash, S., Prakash, L., and Aggarwal, A. K. (2004) Dpo4 Is Hindered In Extending a G-T Mismatch by a Reverse Wobble, *Nat. Struct. Mol. Biol. 11*, 457−462.
29. Morales, J. C., and Kool, E. T. (2000) Functional Hydrogen-Bonding Map of the Minor Groove Binding Tracks of Six DNA Polymerases, *Biochemistry 39*, 12979−12988.
30. Jezewska, M. J., Galletto, R., and Bujalowski, W. (2003) Rat Polymerase β Gapped DNA Interactions Antagonistic Effects of the 5′ Terminal PO^{-4} Group and Magnesium On the Enzyme Binding to the Gapped DNAs With Different ssDNA Gaps, *Cell Biophys. Biochem. 38*, 125−160.
31. Jezewska, M. J., Rajendran, S., Galletto, R., and Bujalowski, W. (2001) Kinetic Mechanisms of Rat Polymerase β-ssDNA Interactions Quantitative Fluorescence Stopped-Flow Analysis of the Formation of the $(\text{Pol }\beta)_{16}$ and $(\text{Pol }\beta)_5$ Binding Mode, *J. Mol. Biol. 313*, 977−1002.
32. Rajendran, S., Jezewska, M. J., and Bujalowski, W. (2001) Multiple-Step Kinetic Mechanisms of the ssDNA Recognition Process by Human Polymerase β in Its Different ssDNA Binding Modes, *Biochemistry 40*, 11794−11810.
33. Jezewska, M. J., Galletto, R., and Bujalowski, W. (2002) Dynamics of Gapped DNA Recognition by Human Polymerase β, *J. Biol. Chem. 277*, 20316−20327.
34. Edelhoch, H. (1967) Spectroscopic Determination of Tryptophan and Tyrosine in Proteins, *Biochemistry 6*, 1948−1954.
35. Gill, S. C., and von Hippel, P. H. (1989) Calculation of Protein Extinction Coefficients From Amino Acid Sequence Data, *Anal. Biochem. 182*, 319−326.
36. Jezewska, M. J., Rajendran, S., and Bujalowski, W. (1998) Functional and Structural Heterogeneity of the DNA Binding of the *E. coli* Primary Replicative Helicase DnaB protein, *J. Biol. Chem. 273*, 9058−9069.
37. Jezewska, M. J., Rajendran, S., Bujalowska, D., and Bujalowski, W. (1998) Does ssDNA Pass Through the Inner channel of the Protein Hexamer in the Complex with the *E. coli* DnaB Helicase? Fluorescence Energy Transfer Studies, *J. Biol. Chem. 273*, 10515−10529.
38. Bujalowski, W., and Jezewska, M. J. (1995) Interactions of *Escherichia coli* Primary Replicative Helicase DnaB Protein with Single-Stranded DNA. The Nucleic Acid Does Not Wrap Around the Protein Hexamer, *Biochemistry 34*, 8513−8519.
39. Jezewska, M. J., Kim, U.-S., and Bujalowski, W. (1996) Binding of *Escherichia coli* Primary Replicative Helicase DnaB Protein to Single-Stranded DNA. Long-Range Allosteric Conformational Changes within the Protein Hexamer, *Biochemistry 35*, 2129−2145.
40. Jezewska, M. J., Rajendran, S., and Bujalowski, W. (1998) Complex of *Escherichia coli* Primary Replicative Helicase DnaB Protein with a Replication Fork. Recognition and Structure, *Biochemistry 37*, 3116−3136.
41. Jezewska, M., Rajendran, S., and Bujalowski, W. (2000) *Escherichia coli* Helicase PriA Protein-Single Stranded DNA Complex, *J. Biol. Chem. 275*, 27865−27873.
42. Jezewska, M., Rajendran, S., and Bujalowski, W. (2000) Interactions of *Escherichia coli* Replicative Helicase PriA Protein with Single-Stranded DNA, *Biochemistry 39*, 10454−10467.
43. Bujalowski, W., and Jezewska, M. J. (2000) in *Spectrophotometry & Spectrofluorimetry. A Practical Approach* (Gore, M. G., Ed.) pp 141−165, Oxford University Press, Oxford.
44. Jezewska, M. J., and Bujalowski, W. (1996) A General Method of Analysis of Ligand Binding to Competing Macromolecules Using the Spectroscopic Signal Originating from a Reference Macromolecule Application to *Escherichia coli* Replicative Helicase DnaB Protein-Nucleic Acid Interactions, *Biochemistry 35*, 2117−2128.
45. Galletto, R., and Bujalowski, W. (2002) The *E. coli* Replication Factor DnaC Protein Exists in Two Conformations with Different Nucleotide Binding Capabilities I. Determination of the Binding Mechanism Using ATP and ADP Fluorescent Analogues, *Biochemistry 41*, 8907−8920.

46. Jezewska, M. J., Galletto, R., and Bujalowski, W. (2004) Interactions of the RepA Helicase Hexamer of Plasmid RSF1010 With the ssDNA. Quantitative Analysis of Stoichiometries, Intrinsic Affinities, Cooperativities, and Heterogeneity of the Total ssDNA-Binding Site, *J. Mol. Biol. 343*, 115−136.
47. Lohman, T. M., and Bujalowski, W. (1991) Thermodynamic Methods for Model-Independent Determination of Equilibrium Binding Isotherms for Protein-DNA Interactions: Spectroscopic Approaches to Monitor Binding, *Methods Enzymol. 208*, 258−290.
48. Baker, B. M., Vanderkooi, J., and Kallenbach, N. R. (1978) Base Stacking In a Fluorescent Dinucleoside Monophosphate: ϵApϵA, *Biopolymers 17*, 1361−1372.
49. Tolman, G. L., Barrio, J. R., and Leonard, N. J. (1974) Chloroacetaldehyde-Modified Dinucleoside Phosphates Dynamic Fluorescence Quenching and Quenching Due to Intramolecular Complexation, *Biochemistry 13*, 4869−4878.
50. McGhee, J. D., and von Hippel, P. H. (1974) Theoretical Aspects of DNA - Protein Interactions Cooperative and Noncooperative Binding of Large Ligands to a One-Dimensional Homogeneous Lattice, *J. Mol. Biol. 86*, 469−489.
51. Epstein, I. R. (1978) Cooperative and Non-cooperative Binding of Large Ligands to a Finite One-Dimensional Lattice. A Model For Ligand - Oligonucleotide Interactions, *Biophys. Chem. 8*, 327−339.
52. Bujalowski, W., Lohman, T. M., and Anderson, C. F. (1989) On the Cooperative Binding of Large Ligands to a One-Dimensional Homogeneous Lattice The Generalized Three-State Lattice Model, *Biopolymers 28*, 1637−1643.
53. Record, M. T., Lohman, T. M., and deHaseth, P. L. (1976) Ion Effects On Ligand - Nucleic Acid Interactions, *J. Mol. Biol. 107*, 145−158.
54. Record, M. T., Jr., Anderson, C. F., and Lohman, T. M. (1978) Thermodynamic Analysis of Ion Effects On the Binding and Conformational Equilibria of Proteins and Nucleic acids the Roles of Ion Association or Release, Screening, and Ion Effects on Water Activity, *Q. Rev. Biophys. 11*, 103−178.
55. Joyce, K. M., and Benkovic, S. J. (2004) DNA Polymerase Fidelity: Kinetics, Structure, and Checkpoints, *Biochemistry 43*, 14317−14324.
56. Galletto, R., Jezewska, M. J., and Bujalowski, W. (2004) Multi-Step Sequential Mechanism of *E. coli* Helicase PriA Protein - ssDNA Interactions Kinetics and Energetics of the Active ssDNA-Searching Site of the Enzyme, *Biochemistry 43*, 11002−11016.
57. Jezewska, M. J., Galletto, R., and Bujalowski. W. (2003) Rat Polymerase β Binds Double-Stranded DNA Using Exclusively the 8-kDa Domain. Stoichiometries, Intrinsic Affinities, and Cooperativities, *Biochemistry 42*, 5955−5970.
58. von, Hippel, P. H., and Schleich T. (1969) in *Structure of Biological Macromolecules* (Timasheff, S., and Fasman G. D., Eds.) pp 417−575, M. Dekker, New York.

BI700677J